STYRELSEN FÖR

VINTERSJÖFARTSFORSKNING

WINTER NAVIGATION RESEARCH BOARD

Research Report No 27

ON PLASTIC DESIGN OF AN ICE-STRENGTHENED FRAME

BY VARSTA P., DROUMEV I. V., HAKALA M.

Sjöfartsstyrelsen
Finland

Finnish Board of Navigation

Sjöfartsverket
Sverige

Swedish Administration
of Shipping and Navigation

ON PLASTIC DESIGN OF AN ICE-STRENGTHENED FRAME

VARSTA P.[1], DROUMEV I.V.[2], HAKALA M.[1]

ESPOO, OCTOBER 1978

[1] TECHNICAL RESEARCH CENTRE OF FINLAND, SHIP LABORATORY

[2] UNIVERSITY OF MECHANICAL AND ELECTROTECHNICAL ENGINEERING IN VARNA, SHIPBUILDING DEPARTMENT AND VISITING RESEARCHER AT HELSINKI UNIVERSITY OF TECHNOLOGY, LABORATORY OF SHIP DESIGN AND STRUCTURES

F O R E W O R D

The Winter Navigation Research Board presents its research report No 27. This is a study of the behaviour of the frame structure of an ice strengthened ship when the plastic limit load is exceeded. The problem is treated both theoretically and experimentally.

The Winter Navigation Research Board expresses its thanks to the authors and all who have assisted them in the work.

Helsingfors och Norrköping November 1978

Jan-Erik Jansson

Lennart Johansson

ABSTRACT

Plastic design methods are applied to determine the load carrying capacity of the shell structure of an ice-going ship. The main object is the behaviour of the ice-strengthened frame, when the yield stress level is reached and exceeded. In the first part of this report quite simple analytical methods are used to study the various collapse mechanisms of the frame. The ultimate strength of the individual parts of the frame is determined and the total load carrying capacity is then calculated. The possibility of the lateral collapse of the frame is studied, too.

A non-linear three-dimensional finite element analysis is also carried out to study more exactly the behaviour of the frame and to check the validity of the simple analytical formulas. In the last part of this report, the results of structural model tests are compared with those of the analytical study and the finite element analysis.

CONTENTS

LIST OF SYMBOLS

A	sectional area
A_b	sectional area of bracket
A_f	sectional area of flange
A_p	sectional area of effective plating
A_s	sectional area in shear
A_w	sectional area of web plate
a	length of plate field
b	breadth of plate field
b_e	effective breadth of plating
b_w	effective width of plating
C	constant
E	Young's modulus
E_t	tangent modulus
h	height of web plate
K	constant in buckling analysis
L	span of frame
L_l	height of load
M	bending moment
M_p	plastic moment
M_{ps}	plastic moment including the effect of shear and buckling
M_{pu}	plastic moment including the effect of buckling (ultimate moment)
F	total load
Q	shear force
Q_p	plastic shear force

Q_{pu}	plastic shear force including the effect of buckling
Q_{pub}	ultimate shear force of cross section with bracket
t_f	thickness of effective plating
t_w	thickness of web plate
U	internal energy
v	deflection
W	external work
W_p	plastic section modulus
W_{ps}	plastic section modulus modified to include the effect of shear
w_o	lateral displacement defined in Fig. 10
W_{psb}	plastic section modulus of including bracket and shear
α	angle of cylindrical hinge defined in Fig. 10
α_y	material constant defined in Fig. 2
β	plate slenderness ratio
Δ	constant defined in Eq. 6
δ_1	virtual displacement due to shear force
δ_2	virtual displacement due to bending moment
ε	strain
ε_u	ultimate strain
ε_y	strain corresponding to yielding
κ	constant defined in Eq. 2.a
ν	Poisson's ratio
σ	normal stress
σ_a	average normal stress
σ_{cr}	critical buckling stress
σ_f	stress in flange
σ_e	elastic buckling stress
σ_{es}	normal stress in the edge of plate

σ_u	tensile strength and ultimate strength
σ_w	stress in web
σ_v	stress induced from the resistance of flanges
σ_y	yield point (yield-stress level)
σ_{yf}	yield-stress level of flange
σ_1, σ_2	principal stresses
τ	shear stress
τ_{cr}	critical buckling stress in shear
τ_e	elastic buckling stress in shear
τ_u	ultimate shear stress
τ_y	shear yield stress
ϕ	angle of web plate defined in Fig. 4
	angle of principal stresses defined in Fig. 8

1. INTRODUCTION

Structural design is normally based on two factors: load or today called demand, and strength today called capacity. Thus the design of a structural system should consist of the determination of relevant load history and corresponding strength criterias.

The results of full-scale measurements /1, 2/ and also the analysis of ice-damages /3/ indicate that the stresses in a transverse ice-strengthened frame are not alternating, i.e. they are always of the same sign. Owing to this the criteria of the plastic limit strength is one of the decisive criterias with which an optimal structure for the life time of an ice-going ship can be achieved.

For instance, when the plating with transverse framing is concerned, the measurements show that the question of strength criterias is more complicated as the stresses have to be considered alternating.

Of course also other important criterias exist, which may determine the limit of structural usefulness of an ice-going ship, such as excessive deflections, fatique and fracture in low temperature.

Plastic design itself has some practical advantages compared to the design based on the criteria of yield strength (allowable stress). This criteria emphasizes the importance of stress rather than strength. The plastic design does not do this. The secondary stresses, which always appear in a structure, do not have any influence on plastic limit load when the material used is ductile. On the contrary, these secondary stresses introduce complexity to the calculations when the criteria of yield strength is used, which is unnecessary for many structural problems in a ship.

This report deals with the theoretical and experimental study on the structural behaviour of the transverse framing of an ice-going ship, when plastic limit load is reached and exceeded. This aims of this study are the following:

- application of the ultimate theorems to predict the load carrying capacity of an ice-strengthened frame

- to achieve insight into the possibilities of applying non-linear finite element analysis to the problem in question

- to compare theoretical and experimental results

- to obtain an idea on how the structure behaves when the plastic limit load is exceeded.

2. A MODEL OF AN ICE-STRENGTHENED SHELL

The shell structure of an ice-going ship normally consists of plating, frames, stringers and webframes. This configuration gives a flexible structure and also a possibility of obtaining light construction. Intermediate frames are used to avoid a too big increase in the thickness of shell plating. The frames are normally fitted perpendicular to the centre line of the ship and equipped with brackets.

For the study described in reference /4/ a structural model was built representing an ice-strengthened shell structure of a ship intended for polar regions. This model is used as a basis for the practical calculations made in this report in spite of the fact that the model has some features which are unnecessary from a point of view of the theoretical study.

A sketch of the model is shown in Fig. 1. It has been scaled from the shell structure of an icebreaker and at the same time modified for some practical reasons. Owing to this the model eather represents the shell structure of an ice-strengthened merchant ship. The structure surrounding the loaded frame has also been included. The frames are made from T-profile which gives good possibilities to get an optimum cross section. The angle between the web plate of the frame and the plating is 20^{o}.

The configuration of load is also shown in Fig. 1. The height of the load was kept as a parameter and therefore it is not equal to the span of the frame. The pressure on the load area is supposed to be distributed uniformly.

To get information about the real strength values of the material, tensile tests were made on four samples taken from the model. The results are given in reference /5/. On the basis of these tests the strength values shown in Table 1 were chosen for the calculations.

Element	Strength group	Yield point σ_y (N/mm^2)	Tensile strength σ_u (N/mm^2)	Maximum elongation (%)
plating	MS	260	420	38.6
flange of fr.	36	410	580	33.6
web plating of fr.	36	440	590	31.5
brackets of fr.	36	440	590	31.5

Table 1. Strength values of the frame elements.

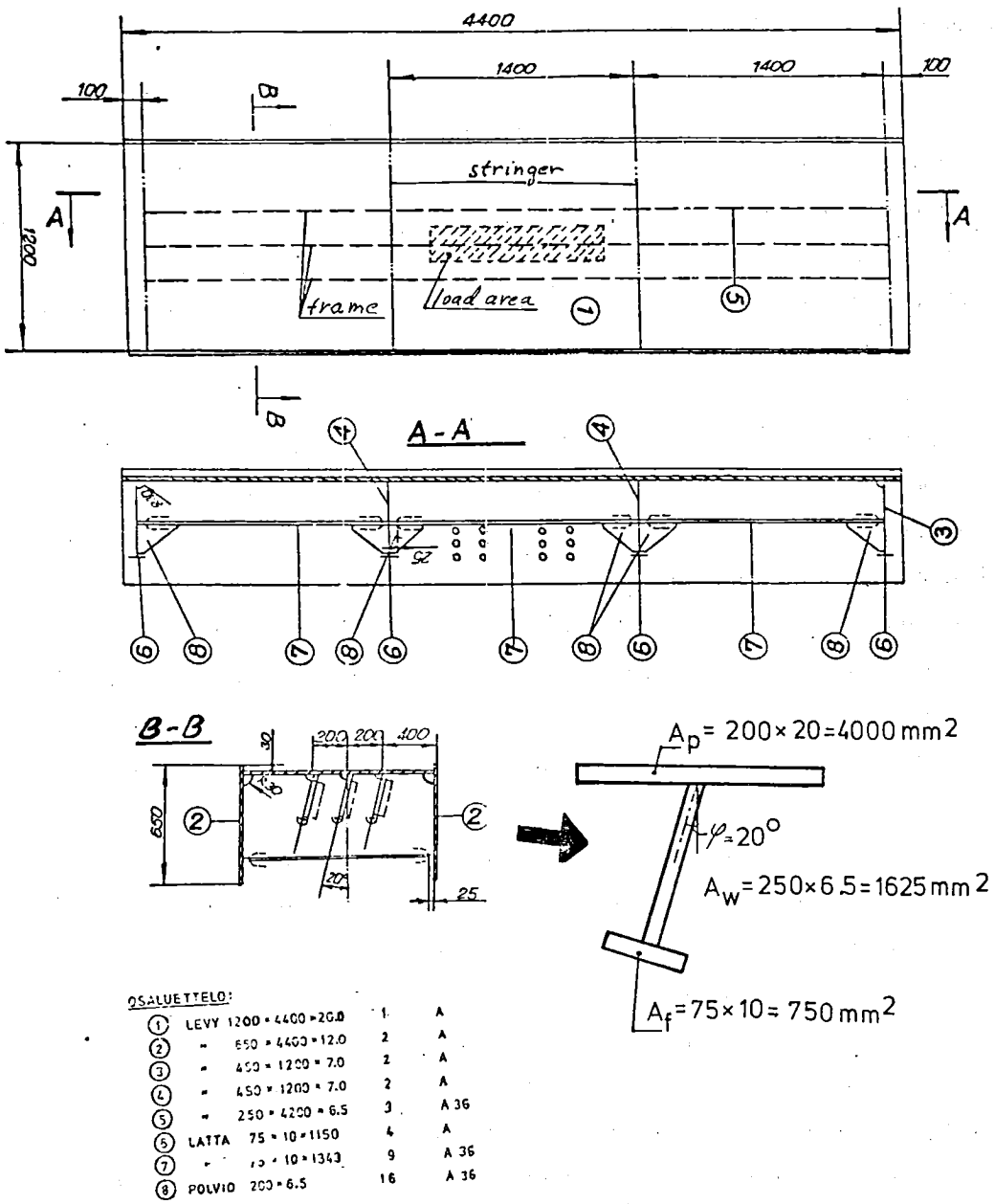

Fig. 1. A sketch of the model of an ice-strengthened shell structure.

3. PLASTIC LIMIT LOAD OF THE FRAME

3.1 Assumptions and definitions

It is assumed that the material of the structure is elastic-perfectly plastic and it is ductile having a capacity to undergo plastic deformation without fracture. The stress-strain curve is shown in Fig. 2. In bending and shear the material follows the solid line. For the buckling analysis, the dashed line is used.

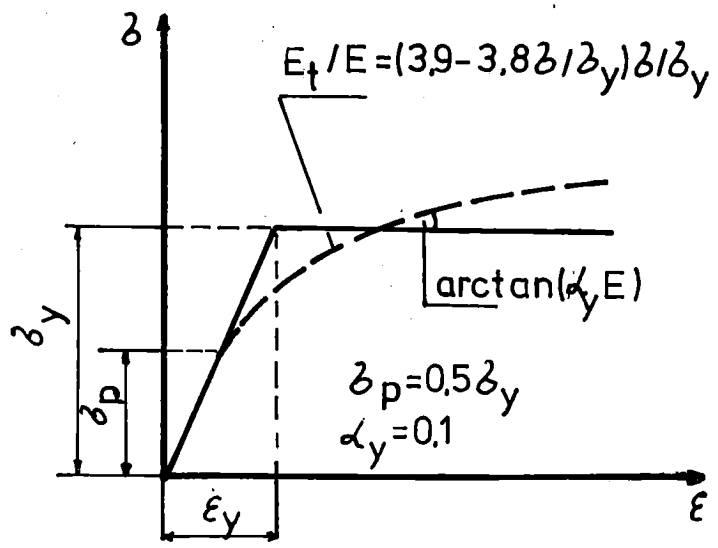

Fig. 2. The stress strain curves
solid line is used in bending and shear
dashed line is used in buckling analysis

A plastic hinge means a hypothetical ultimate stress distribution in the cross section of a beam. In this state the cross section can not carry more load and acts like a mechanical hinge restrained by the plastic moment. Fig. 3 shows the development of a plastic hinge in bending and in shear then called a slipping hinge, for a rectangular bar. In this study it is supposed that normal force is absent.

The ultimate stress in the plastic hinge is either yield stress or ultimate buckling stress depending on which one is reached first. In the buckling analysis the elements of the cross section are considered plates.

The plastic limit load is reached when there is a sufficient number of plastic hinges to create a mechanism. It is supposed that the load is increased gradually.

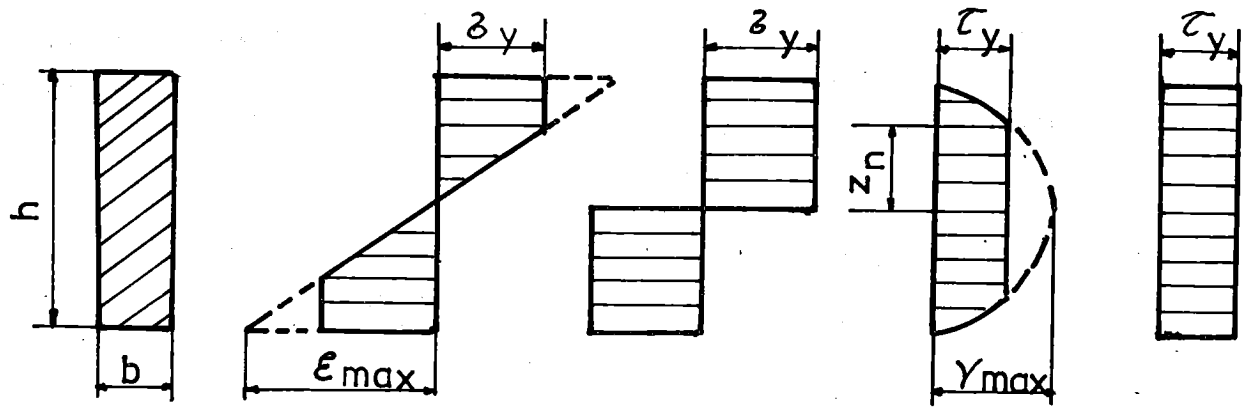

Fig. 3. The normal and shear stress distributions at elastic-plastic and plastic phases for a rectangular profile.

A = bh $\quad M/M_p = 1 - 1/3\zeta^2 \quad \zeta = \varepsilon_y/\varepsilon_{max} \quad M_p = \sigma_y bh^2/4$

$$Q/Q_p = 2/3 \left[2z_n/h + 1/(1 + 2z_n/h) \right]$$

$$Q_p = \tau_y A$$

3.2 Sectional load carrying capacity

3.2.1 Plastic moment

As mentioned earlier, plastic moment M_p or plastic shear force Q_p is reached through the plasticization of the cross section. The following formulae are used in this connection:

$$M_p = \sigma_y W_p \qquad (1.a)$$

$$Q_p = \tau_y A_s$$

where σ_y = yield stress
W_p = plastic section modulus
τ_y = yield stress in shear
A_s = sectional area in shear

However the first formula in Eq.1.a ignores the effect of shear force on the plastic moment and it may also be possible that the yield-stress level is not reached as the elements in compression buckle before. In this case, the following notations are used:

$$M_{pu} = \sigma_u W_p \qquad \text{when } Q = 0$$

$$M_{ps} = \sigma_u W_{ps} \qquad \text{when } Q \neq 0 \qquad (1.b)$$

$$Q_{pu} = \tau_u A_s \qquad \text{when } M = 0$$

where M_{pu} = plastic moment including the effect of buckling
M_{ps} = plastic moment including the effect of shear and buckling
M = bending moment
Q = shear force
Q_{pu} = plastic shear force including the effect of buckling
W_{ps} = plastic section modulus modified to include the effect of shear
σ_u = ultimate normal stress ($\sigma_u \leq \sigma_y$)
τ_u = ultimate shear stress ($\tau_u \leq \tau_y$)

The plastic moment and shear force depend (see Eq. 1) firstly on the geometrical properties of the cross section including also the effect of possible shear and secondly on the ultimate strength of the elements of the cross section, where of course the effect of post-buckling behaviour has been taken into account.

The previous formulae loose their validity if the demand of rigidity of the frame against lateral collapse (tripping) is not fullfilled. That is why the critical angle of the web plate has to be determined, too.

3.2.2 Plastic section modulus

As it is known, the plastic section modulus W_p is the first moment of area of the cross section of a beam about the plastic neutral axis. For a T-profile shown in Fig. 4 the formulae of the plastic section modulus are as follows:

$$\text{if } A_p \leq A_f + A_w$$

$$W_p = \kappa h(A_f + 0.5\, A_w) + 0.5(A_f t_f + A_p t_p) \qquad (2.a)$$

$$\text{where } \kappa = 1 - \frac{A_w}{A_f + 0.5\, A_w}\left(\frac{A_f + A_w - A_p}{2A_w}\right)^2$$

$$\text{if } A_p \geq A_f + A_w$$

$$W_p = h(A_f + 0.5A_w) + 0.5\,(A_f T_f + A_p t_p) - \qquad (2.b)$$

$$- \frac{1}{4}\frac{t_p}{A_p}(A_f + A_w - A_p)^2$$

The meaning of the symbols is shown in Fig. 4. If the elements of the profile are of a material which has different yield-stress levels, the effect of these elements on the section modulus has to be reduced in the proportion of the ratio between yield points. When the frame is not fitted perpendicular to the plating the following reductions have to be made:

$$h' = h\cos\phi \tag{3}$$

$$t'_f = f_f\cos\phi$$

where angle ϕ is shown in Fig. 4.

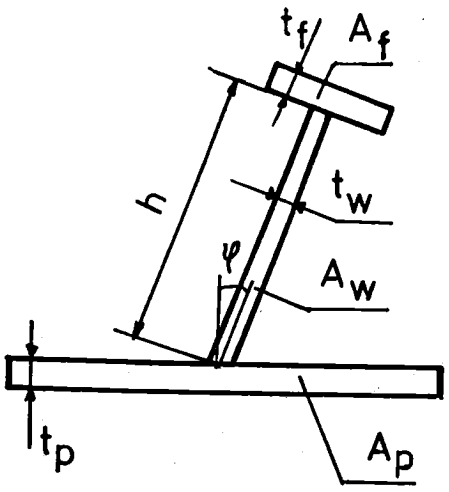

Fig. 4. The elements of a T-profile frame.

The above formula of the plastic section modulus has been derived under the assumption that only pure bending takes place at the plastic hinge. Normally if shear exists at the cross section its effect on the plastic moment has to be taken into consideration. Assuming that the shear stress is uniformly distributed on the web plate and applying von Mises' yield criteria an expression for the rediced normal stress distribution shown in Fig. 5 can be derived in the following way:

from von Mises' yield criteria

$$\sigma_y^2 = \sigma^2 + 3\tau^2 \tag{4}$$

where σ_y = yield point
σ = normal stress
τ = shear stress

We get the expression of the normal stress in the web plate, which can be written as follows:

$$\sigma = \sigma_u \sqrt{1 - \left(\frac{Q}{Q_{pu}}\right)^2} \qquad (5)$$

where $Q = \tau A_s$

$Q_{pu} = \tau_u A_s$ $(Q_{pu} \leq Q_p = \tau_y A_s)$

$\tau_y = \frac{\sigma_y}{\sqrt{3}}$

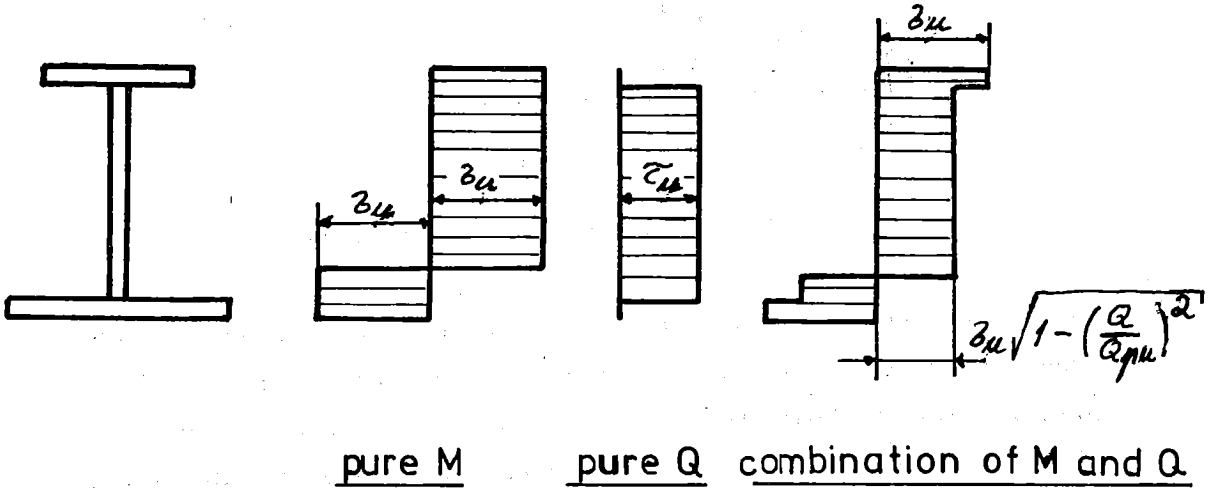

Fig. 5. The distribution of the normal stress when shear is present.

When calculating the plastic section modulus this effect is taken into account by reducing the area of the web plate in the following way:

$$A_w' = A_w \sqrt{1 - \left(\frac{Q}{Q_{pu}}\right)^2}$$

Hence the expression for the plastic section modulus modified to include the effect of shear becomes the following:

$$\kappa\left(\frac{W_{ps}}{W_p}\right) = 1 - \frac{A_w}{2A_f + A_w}\left(1 - \sqrt{1 - \left(\frac{Q}{Q_{pu}}\right)^2}\right) - \Delta \quad (6)$$

where $$\Delta = \frac{A'_w}{A_f + 0.5A_w}\left(\frac{A_f + A'_w - A_p}{2A'_w}\right)^2$$

when $A_f + A'_w > A_p$

and

$\Delta = 0$

when $A_f + A'_w \leq A_p$

3.2.3 Ultimate strength in compression

In order to determine the value of the plastic moment it has to be known what is the ultimate stress of the elements of the cross section. Of course the elements in tension have an ultimate stress value equal to the yield point. For the elements in compression the question is not so simple as they may buckle before reaching the yield-stress level.

As is known, a plate can carry additional load after buckling, if the supporting elements at the plate edges are stiff enough. The theoretical solution of the postbuckling strength does not give good results compared with the empirical formulae based on tests. However, the problem can be studied using the hypothesis of equivalet contour /6/. The principle of this hypothesis is shown in Fig. 6.a. For the evaluation of the ultimate strength of a long plate a square one can be studied.

Using the energy method, a formula for the ultimate strength in compression can be derived. The following expressions for the internal energy and external work can be obtained from Fig. 6:

Internal energy $U = -\left[\sigma_{es} b_f t(b\varepsilon_{es}) + \sigma_{es}(b - b_f)t(a_f\varepsilon_{es})\right]$

External work $W = \sigma_{es} b_w t(b\varepsilon_{es}) = \sigma_a b t(b\varepsilon_{es})$

where b_w = effective width of plating
σ_{es} = edge stress
σ_a = average stress

The meaning of the other quantities can be found in Fig, 6.b.

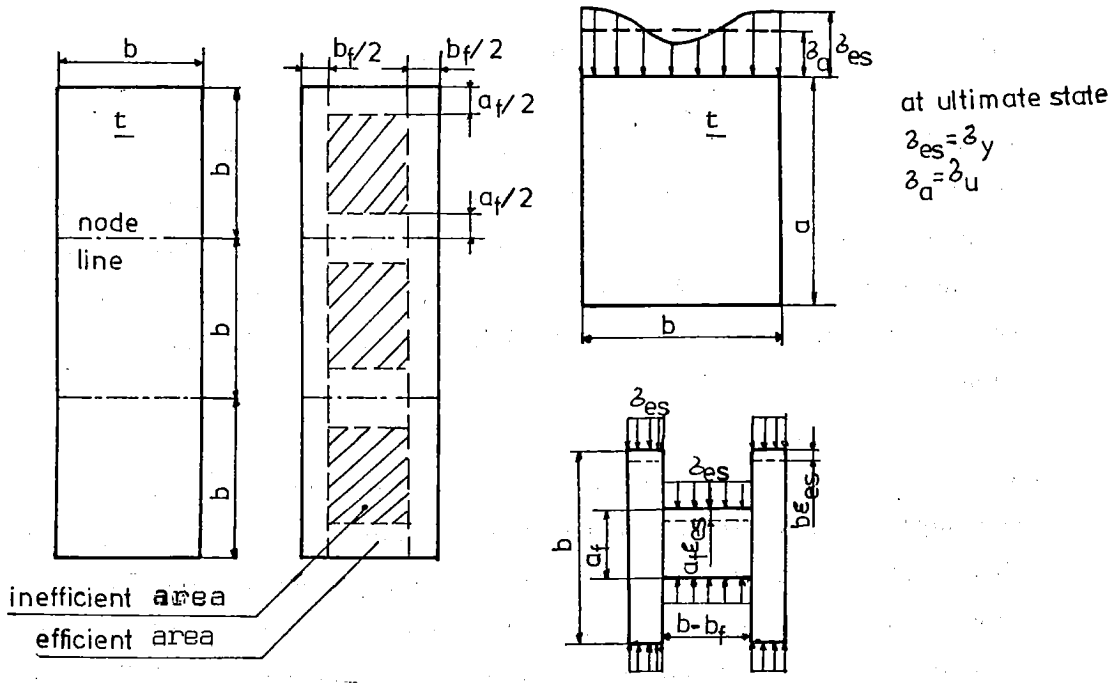

Fig. 6. Ultimate strength of a plate in compression, the hypothesis of equivalent contour.

Minimizing the total potential energy, i.e.

$$\frac{\partial U}{\partial \varepsilon_{es}} + \frac{\partial W}{\partial \varepsilon_{es}} = 0$$

the following expression for the ratio between the effective width and the breadth of the plate is obtained:

$$\frac{b_w}{b} = \frac{\sigma_a}{\sigma_{es}} = \frac{b_f + a_f}{b} - \frac{b_f a_f}{b^2}$$

At the ultimate stage

$$\sigma_{es} = \sigma_y$$

$$\sigma_a = \sigma_u$$

and consequently

$$\frac{\sigma_u}{\sigma_y} = \frac{b_f + a_f}{b} - \frac{b_f a_f}{b^2}$$

Using a parameter called slenderness ratio β, the previous equation can be written in the following form:

$$\frac{\sigma_u}{\sigma_y} = \frac{\beta_b + \beta_a}{\beta} - \frac{\beta_b \beta_a}{\beta^2} \qquad (7)$$

where $\beta = \frac{b}{t}\sqrt{\frac{\sigma_y}{E}}$ = plate slenderness ratio

$$\beta_b = \frac{b_f}{t}\sqrt{\frac{\sigma_y}{E}}$$

$$\beta_a = \frac{a_f}{t}\sqrt{\frac{\sigma_y}{E}}$$

The slenderness ratios β_a and β_b should be determined experimentally. Assuming that they are equal and solving the slenderness ratio from the formula of the elastic buckling stress of a plate, which is

$$\frac{\sigma_e}{\sigma_y} = \frac{K\pi^2}{12(1-\nu^2)} \cdot \frac{1}{\beta^2} \qquad (8)$$

where σ_e = elastic buckling stress

K = constant depending on the boundary conditions

Eq. 7 can be written in the following way

$$\frac{\sigma_u}{\sigma_y} = 2\sqrt{C\frac{\sigma_e}{\sigma_y}} - C\frac{\sigma_e}{\sigma_y} \text{ when } C\frac{\sigma_e}{\sigma_y} \leq 1 \qquad (9)$$

where $C = \frac{\beta_b^2}{K}\frac{12(1-\nu)^2}{\pi^2}$

The constant C can be solved by fitting the curve of Eq. 9 to that of the critical buckling stress σ_{cr}, which is /6/:

$$\sigma_{cr} = \frac{3.9\sigma_e^2}{3.8\sigma_e^2+\sigma_y^2}\sigma_y \qquad \text{when } 0.5 \leq \frac{\sigma_e}{\sigma_y} \leq \sqrt{10} \qquad (10)$$

$$\sigma_{cr} = \sigma_y \qquad \text{when } \frac{\sigma_e}{\sigma_y} \geq \sqrt{10}$$

$$\sigma_{cr} = \sigma_e \qquad \text{when } \frac{\sigma_e}{\sigma_y} \leq 0.5$$

Eq. 10 is based on the deformation theory of plasticity and on the stress-strain curve shown in Fig. 2. The curves of Eq. 9 and Eq. 10 with C = 0.341 for a simply supported square plate are shown in Fig. 7. The curve of the critical buckling stress by Johnson-Ostenfeld and that of the ultimate strength by Faulkner /9/ are also shown there.

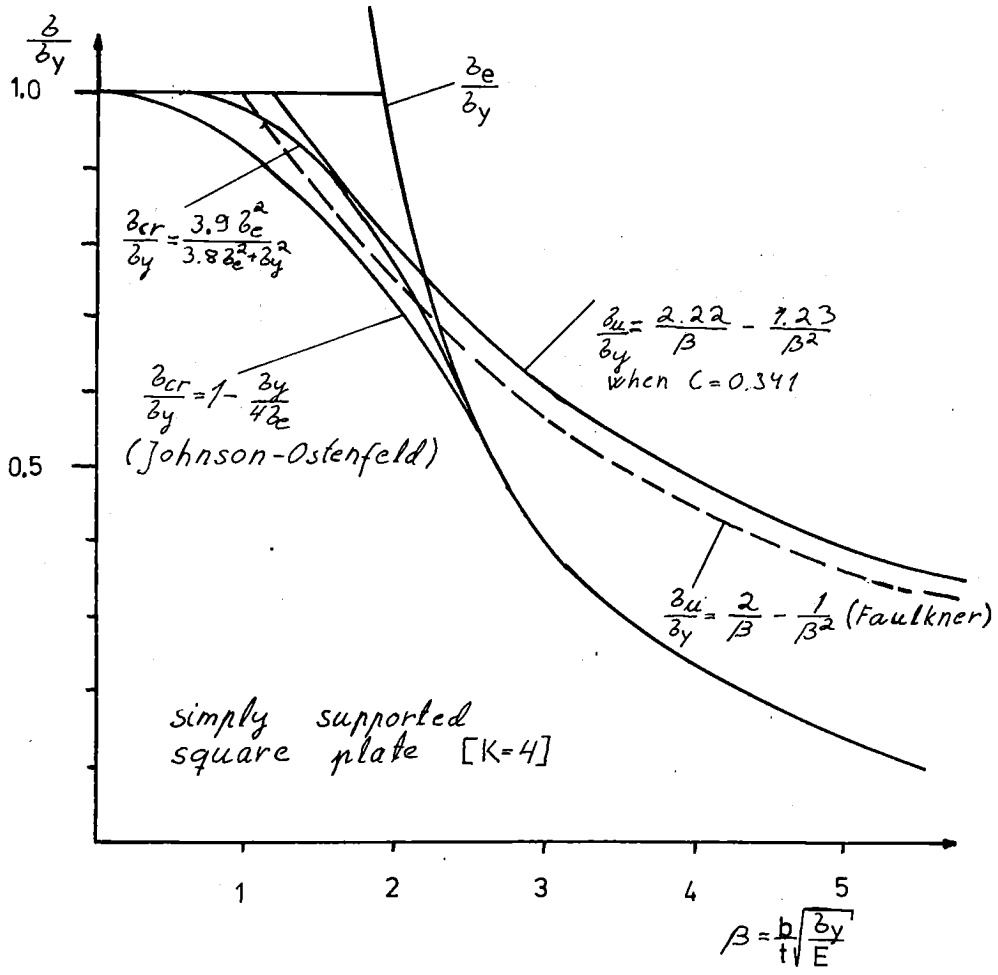

Fig. 7. Buckling strength of a plate in compression as a function of the slenderness ratio.

3.2.4 Ultimate strength in shear

The loading pattern is shown in Fig. 8. It is supposed that the only external load is the shear force Q. From the theory of elasticity the following expressions are obtained:

$$\sigma_1 = \tau \sin 2\phi$$
$$\sigma_2 = -\tau \sin 2\phi \qquad (11)$$

where $\tau = Q/(ht)$

σ_1 and σ_2 = principal stresses

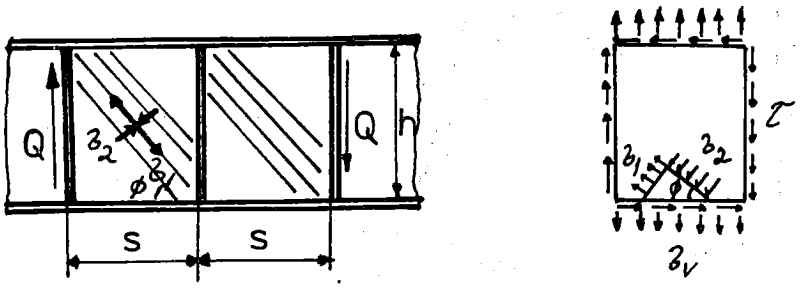

Fig. 8. Buckling of a plate in shear.

At the ultimate state the principal stress σ_2 is

$$\sigma_2 = (\sigma_2)_{cr} = -\tau_{cr} \sin 2\phi \tag{12}$$

where τ_{cr} = critical buckling stress in shear

Using the hypothesis of maximum shear stress the yield condition has the following form:

$$|\sigma_1 - \sigma_2| = \sigma_y = 2\tau_y \tag{13}$$

Forming the equantions of balance of the stresses shown in Fig. 8 the following expressions are obtained:

$$\begin{aligned} \sigma_1 \sin^2\phi + \sigma_2 \cos^2\phi &= \sigma_v \\ (\sigma_1 - \sigma_2) \sin\phi\cos\phi &= \tau_u \end{aligned} \tag{14}$$

where σ_v=stress induced by the resistance of the flanges.

Eqs. 13 and 14b give the following expression for the ratio τ_u/τ_y:

$$\frac{\tau_u}{\tau_y} = \sin 2\phi \qquad (15)$$

The formula of the ratio σ_v/σ_y is obtained from Eqs. 12, 13 and 14.a:

$$\frac{\sigma_v}{\sigma_y} = \sin^2\phi - 0.5 \frac{\tau_{cr}}{\tau_y} \sin 2\phi \qquad (16)$$

Using the trigonometric formula

$$\sin\phi = \frac{1}{2}\sqrt{1 + \sin 2\phi} - \frac{1}{2}\sqrt{1 - \sin 2\phi}$$

and ignoring the normal stress σ_v the following expression for the ultimate shear stress τ_u can be derived from Eqs. 15 and 16:

$$\frac{\tau_u}{\tau_y} = \frac{2\,\tau_{cr}/\tau_y}{1+\left(\frac{\tau_{cr}}{\tau_y}\right)^2} \qquad (17)$$

where

$$\frac{\tau_{cr}}{\tau_y} = \frac{3.9(\tau_e/\tau_y)^2}{3.8(\tau_e/\tau_y)^2 + 1} \quad \text{when } 0.5 \leq \frac{\tau_e}{\tau_y} \leq \sqrt{10}$$

$$\frac{\tau_{cr}}{\tau_y} = 1 \quad \text{when } \frac{\tau_e}{\tau_y} \geq \sqrt{10}$$

$$\frac{\tau_{cr}}{\tau_y} = \frac{\tau_e}{\tau_y} \quad \text{when } \frac{\tau_e}{\tau_y} \leq 0.5$$

τ_e = elastic buckling stress in shear

The ultimate shear stress τ_u as a function of the slenderness ratio β is drawn in Fig. 9. The critical buckling stress in shear τ_{cr} is also represented there.

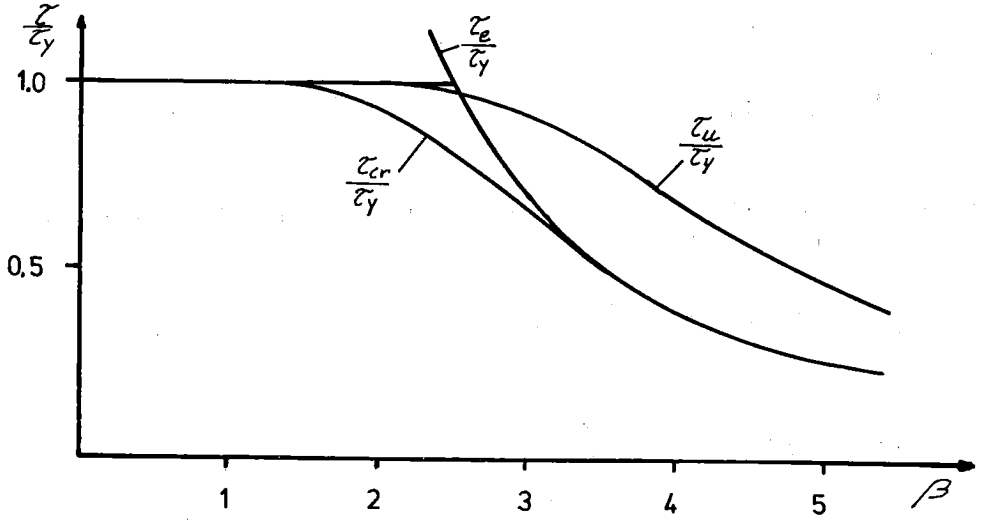

Fig. 9. Ultimate strength of a plate in shear as a function of the slenderness ratio.

3.2.5 On the lateral collapse of the frame

As was described in chapter 3.2.1, the rigidity of the frame against lateral collapse, which could also be called tripping of the frame, has to be studied. A starting point of the study is that the angle between the web plate and the plating differs from the right angle. The vertical load on the plating is the only external force.

The problem is treated using the energy method. It is supposed that the collapse mechanism of the frame is as shown in Fig. 10. The expression of internal plastic energy for a simply supported plate is the following:

$$U = - \frac{t_w^2 \sigma_y w_o}{2 \tan\alpha} \left(\frac{A_f^2 h}{A_w^2 t_f} + 1 + \tan^2\alpha \right) \qquad (18)$$

The meaning of the symbols in Eq. 18 can be found in Fig. 10.

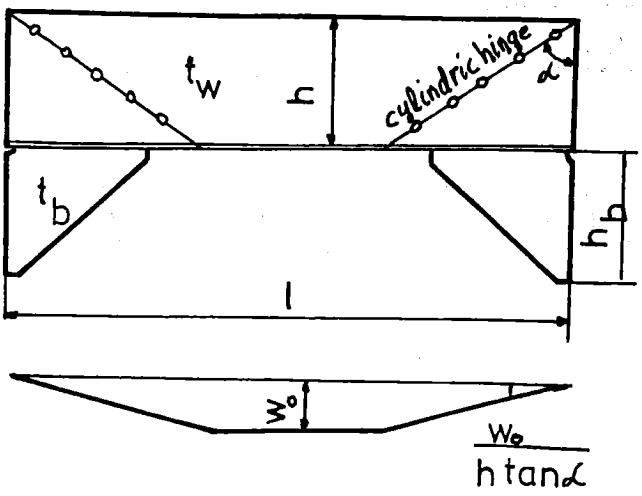

Fig. 10. The lateral collapse mechanism of the frame.

The collapse is caused by a lateral force, which arises because the angle of the normal stress σ_x changes in the direction of the x-axis as Fig. 11 shows. The expression of the transverse force per unit length q_t is obtained from the following moment equation:

$$hq_t = \int_{A_f+A_w} \sigma_b \ (z + h - h_1) \ dA \ \sin\phi$$

where the meaning of the quantities is shown in Fig. 11. This equation can be written in the following form:

$$q_t = \sigma_f (A_f + K A_w) \frac{d^2v}{dx^2} \sin\phi \qquad (19)$$

where q_t = lateral force per unit length
σ_f = bending stress in the flange
K = 0.5 at plastic stage when $A_p \geq A_f + A_w$
v = vertical deflection

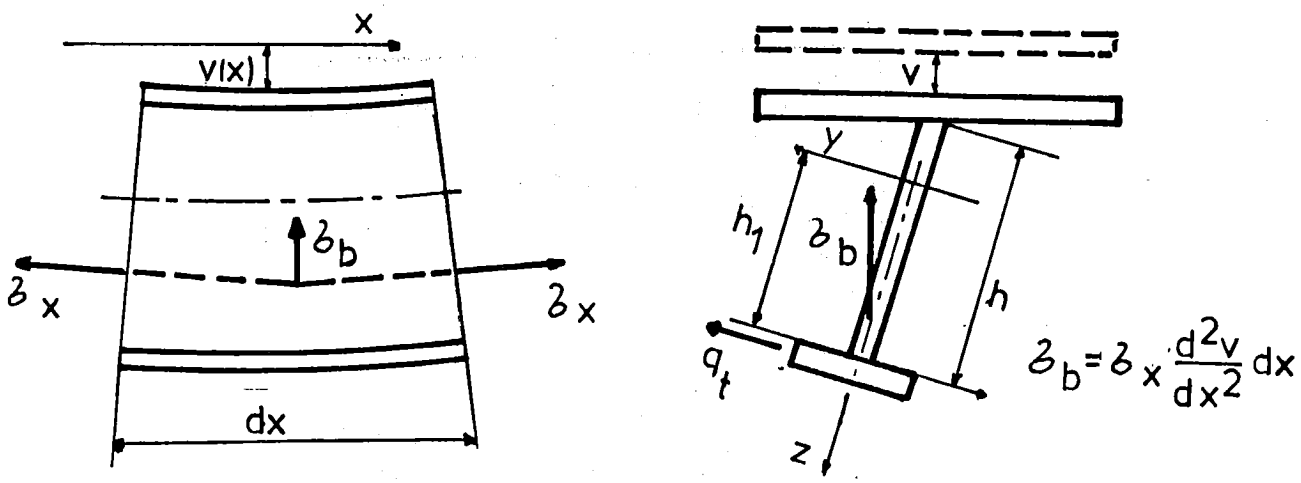

Fig. 11. Formation of transverse force q_t.

If it is assumed that the distribution of the force q_t in the direction of the x-axis is as Fig. 12 shows, then the external work W is:

$$W = q_{to} a w_o - 4/3 q_{to} w_o h \tan\alpha \qquad (20)$$

From the equation

$$\frac{\partial W}{\partial w_o} + \frac{\partial U}{\partial w_o} = 0$$

we get the following inequality

$$q_{to} \leq \frac{1}{a - \frac{4}{3}h\tan\alpha} \frac{t_w^2 \sigma_y}{2\tan\alpha} \left(\frac{A_f^2 h}{A_w^2 t_f} + 1 + \tan\alpha \right) \qquad (21)$$

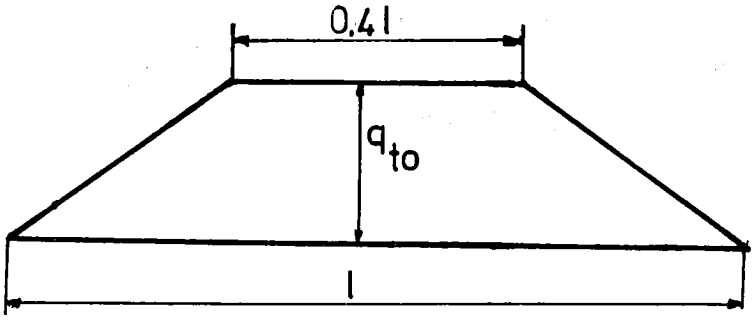

Fig. 12. The distribution of transverse force q_t, simply supported case.

This inequality means that if the force q_{to} is bigger than the value of the right side, lateral collapse will occur. The right side of Eq. 21 obtains its minimum, when the cylindric hinges start from the tip of the brackets and then $\tan\alpha \simeq 1$. Taking into consideration Eq. 10 and that

$$\frac{\partial^2 v}{\partial x^2} \simeq \frac{\varepsilon_f}{h_1}$$

where ε_f = strain in the flange

and that $h_1 \simeq h$ at plastic hinge for a cross section where $A_p \geq A_f + A_w$, Eq. 21 can be written in the following form:

$$\sin\phi \leq \frac{t_w^2 h}{2\varepsilon_f a(1-4h/3a)} \frac{1}{(A_f + 0.5 A_w)} \left(\frac{A_f^2 h}{A_w^2 t_f} + 2 \right)$$

If it is assumed that when the strain in the flange is $\varepsilon_f = 10\varepsilon_y$, strain hardening begins to move the plastic hinges towards the ends of the frame, and the distribution of the load q_t obtains the shape shown in Fig. 12, then the inequality is:

$$\sin\phi \leq \frac{t_w^2 E/\sigma_{yf}}{20a(1-4h/3a)} \frac{1}{(A_f+0.5A_w)} \left(\frac{A_f^2 h}{A_w^2 t_f} + 2 \right) \qquad (22)$$

where σ_{yf} = yield-stress level of flange

3.3 Plastic limit load

The mechanism method is employed to determine the plastic limit load of the frame. It is supposed that there will be two kinds of modes of failure. The first mode is due to the plastic slipping of the ends of the frame. The second mode is caused by the formation of three hinges. The load configuration with possible collapse modes is shown in Fig. 13. Applying the principle of virtual displacements corresponding to failure mechanism it is possible to obtain the expressions of the plastic limit load.

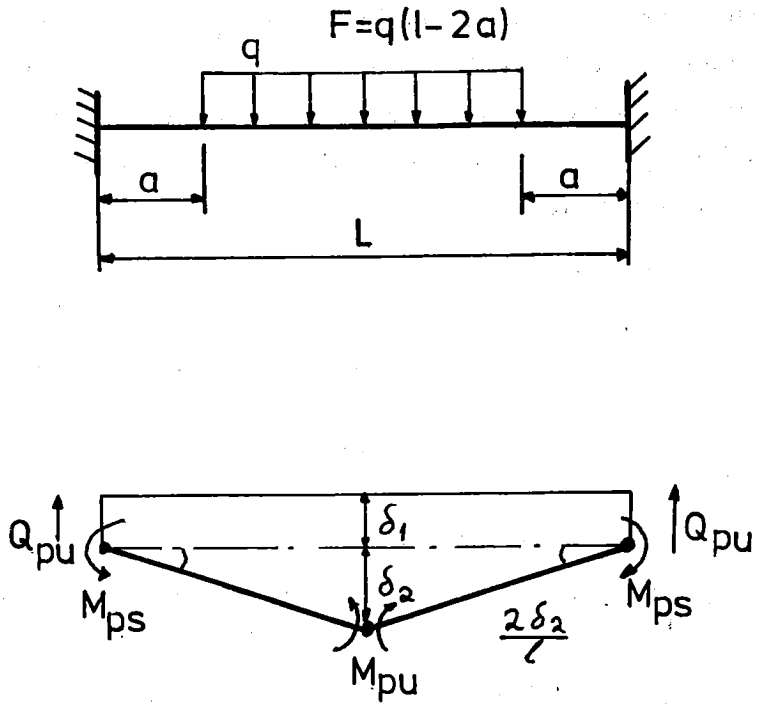

Fig. 13. Load pattern with assumed collapse modes.

The expression of the internal energy on the basis of Fig. 13 is

$$U = - [\ 2Q_{pu}\delta_1 + \frac{4\delta_2}{L}\ (M_{pu} + M_{ps})]$$

where δ_1 and δ_2 are virtual displacements. The work done by the external load is

$$W = F\delta_1 + F\delta_2\ \frac{L + 2a}{2L}$$

when we insert these expressions in the following equations:

$$\frac{\sigma U}{\sigma \delta_i} + \frac{\sigma W}{\sigma \delta_i} = 0,\ i = 1,\ 2$$

the two following formulae for the plastic limit load are obtained:

$$F = 2Q_{pu} \qquad (23)$$

$$F = \frac{8}{L + 2a}\ (M_{pu} + M_{ps}) \qquad (24)$$

The real failure mode will be the one which gives the lowest value of load, because any greater load would lead to the violation of the plastic moment (or shear) condition.

3.4 Calculations of the plastic limit load of the frame

In the following are represented numerical calculations which are based on the previous theory. First the sectional load carrying capacity of the profile is calculated and then value of the plastic limit load of the frame is solved. In this connection the effect of the bracket on the plastic moment is also studied. The dimensions of the structure are shown in Fig. 1.

3.4.1 Ultimate strength of the elements of the cross section

First it has to be checked that the lateral collapse of the frame does not occur. Eq. 22 with the following data:

$$\sigma_{yw} = 440 \text{ N/mm}^2 \qquad A_w = 1625 \text{ mm}^2$$
$$\sigma_{yf} = 410 \text{ N/mm}^2 \qquad t_w = 6.5 \text{ mm}$$
$$a = 1400 \text{ mm} \qquad t_f = 10 \text{ mm}$$
$$h = 250 \text{ mm} \qquad E = 2.06 \cdot 10^5 \text{ N/mm}^2$$

$$A_f' = \frac{\sigma_{yf}}{\sigma_{yw}} A_f = 699 \text{ mm}^2$$

$$A_f = 750 \text{ mm}^2$$

gives $\sin\phi \leq 1.08$

which means that the lateral collapse cannot occur.

The ultimate strength of the different elements of the profile:

Plating

$b = 200$ mm (frame spacing)

$t = 20$ mm

$\sigma_y = 260$ N/mm^2

$$\beta = \frac{b}{t}\sqrt{\frac{\sigma_y}{E}} = 0.36$$

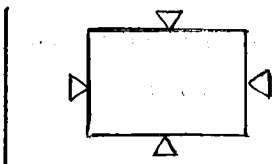

$\Rightarrow$ K=4, $\frac{\sigma_e}{\sigma_y} = 28.4$

Δ = simply supported; $\frac{\sigma_u}{\sigma_y} = 1$ (Eq. 9)

Flange

$b = 37.5$ mm

$t = 10$ mm

$\sigma_y = 410$ N/mm^2

$\beta = 0.17$

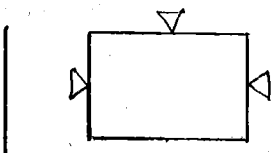

$\Rightarrow$ K = 1.44

$\frac{\sigma_e}{\sigma_y} = 46.1$, $\frac{\sigma_u}{\sigma_y} = 1$ (Eq. 9)

Web plate

$b = 250$ mm

$t = 6.5$ mm

$\sigma_y = 440$ N/mm^2

$\beta = 1.78$

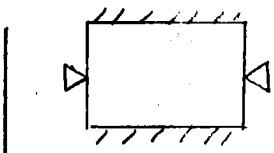

$\Rightarrow$K = 7.69

$\frac{\sigma_e}{\sigma_y} = 2.2$, $\frac{\sigma_u}{\sigma_y} = 0.98 \simeq 1.0$

The ultimate strength in shear for the web plate is:

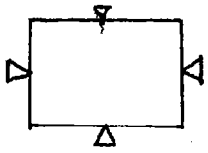

$$K = 5.34\,\frac{\tau_e}{\tau_y} = 264$$

$\frac{\tau_{cr}}{\tau_y} = 0.93$, $\frac{\tau_u}{\tau_y} = 1.0$ (Eq. 17)

3.4.2 Plastic section modulus of the profile

As the angle ϕ is 20^o the height of the web plate and the thickness of the flange have to be reduced using Eq. 3. The reduced values are the following:

$h' = 235$ mm

$t_f' = 9.4$ mm

The yield points of the elements of the cross section are not equal and thus the areas of the flange and the plating have to be reduced, too:

$$A'_f = \frac{\sigma_{yf}}{\sigma_{yw}} A_f = 699 \text{ mm}^2$$

$$A'_p = \frac{\sigma_{yp}}{\sigma_{yw}} A_p = 2364 \text{ mm}^2$$

The area of the web plate remains unchanged being $A_w = 1625$ mm^2.

As $A'_p > A'_f + A_w$ Eq. 2b gives the value of the plastic section modulus

$$W_p = 382 \text{ cm}^3$$

Now the values of the plastic moment and shear force can be calculated from Eq. 1

$$M_{pu} = \sigma_u W_p = \sigma_y W_p = 168.1 \text{ kNm}$$

$$Q_{pu} = \tau_u A_s = \tau_y A_s = \frac{\sigma_y}{\sqrt{3}} A_s = 437 \text{ kN}$$

where $\sigma_y = 440$ N/mm^2

$$A_s = (h + t_f)t_w \cos\phi + t_w t_p = 1718 \text{ mm}^2$$

3.4.3 Plastic limit load of the frame

The frame has three possible failure modes. These are shown in Fig. 14. The first mode is due to shear force. The second and third mode are caused by bending moment. The difference between the second and third one is that in the second case the end hinges appear at the tip of the brackets while in the third case these are at the end of the frame. The true plastic limit load is the smalles value given by these three

assumed failure modes. Using the symbols shown in Fig. 14 the following three equations can be derived from Eq. 23 and 24:

1) $$F = 2Q_{pu}$$

2) $$\frac{FL_1}{8M_{pu}} = 1 + \frac{M_{ps}}{M_{pu}} \qquad (25)$$

3) $$\frac{FL_1}{8M_{pu}} \left(\frac{2L}{L_1} - 1\right) = 1 + \frac{M_{ps}}{M_{pu}}$$

The first mode of collapse gives the following result:

$$F = 874 \text{ kN}$$

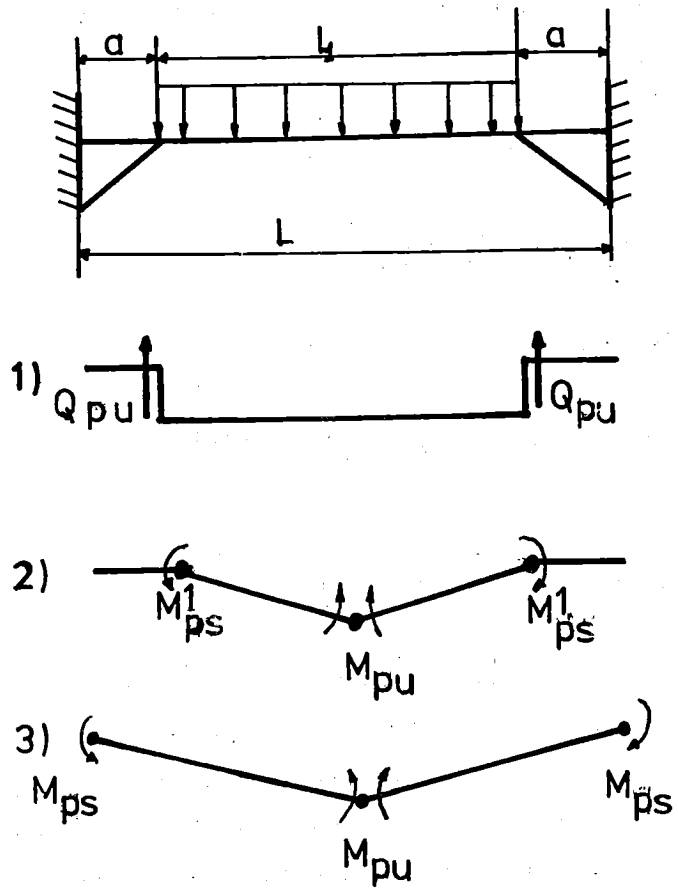

Fig. 14 The possible collapse modes of the frame.

To solve the load of the second mode from Eq. 25.2 this equation has to be modified somewhat. Substituting the following expressions for the left side of the equation:

$$F = 2Q$$

$$M_{pu} = \frac{\sqrt{3}Q_{pu}W_p}{A_s}$$

and for the right side Eq. 6, and also taking into consideration Eqs. 1 and that $\kappa \simeq 1$, the following equation is obtained:

$$c(\frac{Q}{Q_{pu}}) = 2 - d(1 - \sqrt{1 - (\frac{Q}{Q_{pu}})^2}) \qquad (26)$$

where $$c = \frac{A_s L}{4\sqrt{3}W_p}$$

$$d = \frac{A_w}{2A_f' + A_w}$$

From this equation the load of the second mode can be solved. For the frame in question the constants c an d have the following values:

$$c = 0.649$$

$$d = 0.538$$

Inserting these values in Eq. 26 and solving the equation, the roots are found to be imaginary. This means that the second mode cannot occur.

When calculating the load value of the third mode with Eq. 25.3, the effect of brackets on the plastic section modulus has to be taken into account. The distribution of the normal stress including shear effect when the bracket is present is shown in Fig. 15.

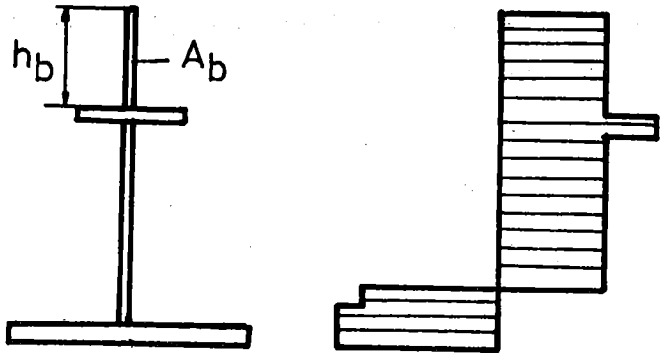

Fig. 15. The distribution of normal stress including the shear force effect when a bracket is present.

In this case the ratio W_{ps}/W_p can be written in the following way:

$$\frac{W_{psb}}{W_p} = 1 - \frac{A_w}{2A_f + A_w}\left\{1 - \left[1+\frac{A_b}{A_w}\left(\frac{h_b}{h} + 2\right)\right]\sqrt{1 - \left(\frac{Q}{Q_{pub}}\right)^2}\right\} \tag{27}$$

where

W_{psb} plastic section modulus including the effect of shear force and bracket

W_p plastic section modulus without the effect of shear and bracket

A_b sectional area of bracket

h_b height of bracket

Q_{pub} ultimate shear force of cross section with bracket

Now using Eq. 27, Eq. 25.3 can be written in the following way:

$$c'\left(\frac{Q}{Q_{pub}}\right)\left(\frac{2L}{L_1} - 1\right) = 2 - d\left[1 - (1 + e)\sqrt{1 - \left(\frac{Q}{Q_{pub}}\right)^2}\right] \tag{28}$$

where $$c' = \frac{(A_s + A_b)L}{4\sqrt{3}\,W_p}$$

$$d = \frac{A_w}{2A_f + A_w}$$

$$e = \frac{A_b}{A_w}\left(\frac{h_b}{h} + 2\right)$$

For the frame in question the constants have the following values:

$$c' = 1.140$$
$$d = 0.538$$
$$e = 2.240$$

Inserting these into Eq. 28 and solving the equation, the following roots are found:

$$\left(\frac{Q}{Q_{pub}}\right)_1 = 0.958$$

$$\left(\frac{Q}{Q_{pub}}\right)_2 = -0.130$$

of which the first one is valid. The value of load is then

$$F = 2\left(\frac{Q}{Q_{pub}}\right)_1 Q_{pub} = 1470 \text{ kN}$$

where $Q_{pub} = 767$ kN

As the load F of the third mode is bigger than that of the first mode, the load value of the first mode gives an estimation of the plastic limit load of the frame.

4. A FINITE ELEMENT ANALYSIS OF THE FRAME

4.1 Introduction

Today computer program packages based on the finite element method are available which make it possible to perform non-linear analyses of complicated structures. The aim of the finite element analysis of the frame in question is twofold, first to get an idea about the possibilities of the FEM-analysis in the problems of this kind, and second to compare the results of this method to those of the analytic study.

In this analysis the program package called ADINA /7/ is used. The element type used includes both material and geometric non-linearity at the same time. The material properties of the frame used at the analysis are shown in Table 1 and a sketch of stress-strain curves is presented in Fig. 16.

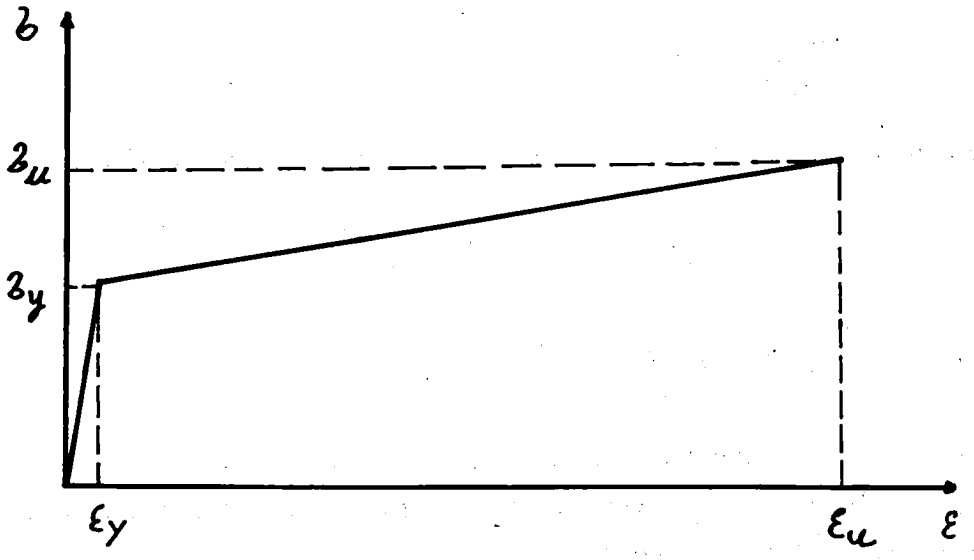

Fig. 16. A sketch of stress-strain curve used in the finite element analysis.

4.2 Description of the finite element model

The element type used is a three dimensional isoparametric thick shell element using total Lagrangian formulation. Elements with 16 and 12 nodal points are used in the element model. The number of integration points in one element is 27. A schematic drawing of this element type is shown in Fig. 17. The displacements of the elements are given at the nodes and stresses at the integration points. In the plastic region, the von Mises' yield conditions is used.

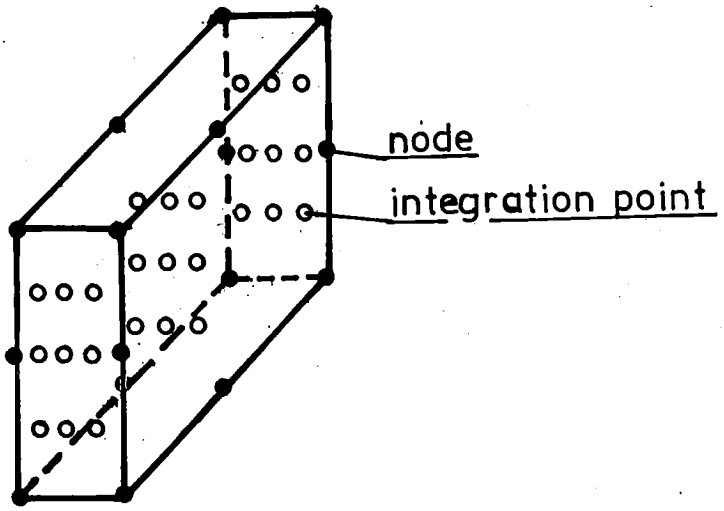

Fig. 17. A sketch of the isoparametric thick shell element.

In this analysis, the main purpose was to study the collapse mechanism of the frame. Owing to this we can restrict ourselves to the loaded frame span as the end constraints do not have any influence on the limit load. Owing to symmetry, only one half of the span of the frame has to be taken into account in the element model. The width of the element mesh is the same as that of the test model, that is 1200 mm. Of the three frames only the middle one with the brackets is included. The element mesh is shown in Fig. 18.

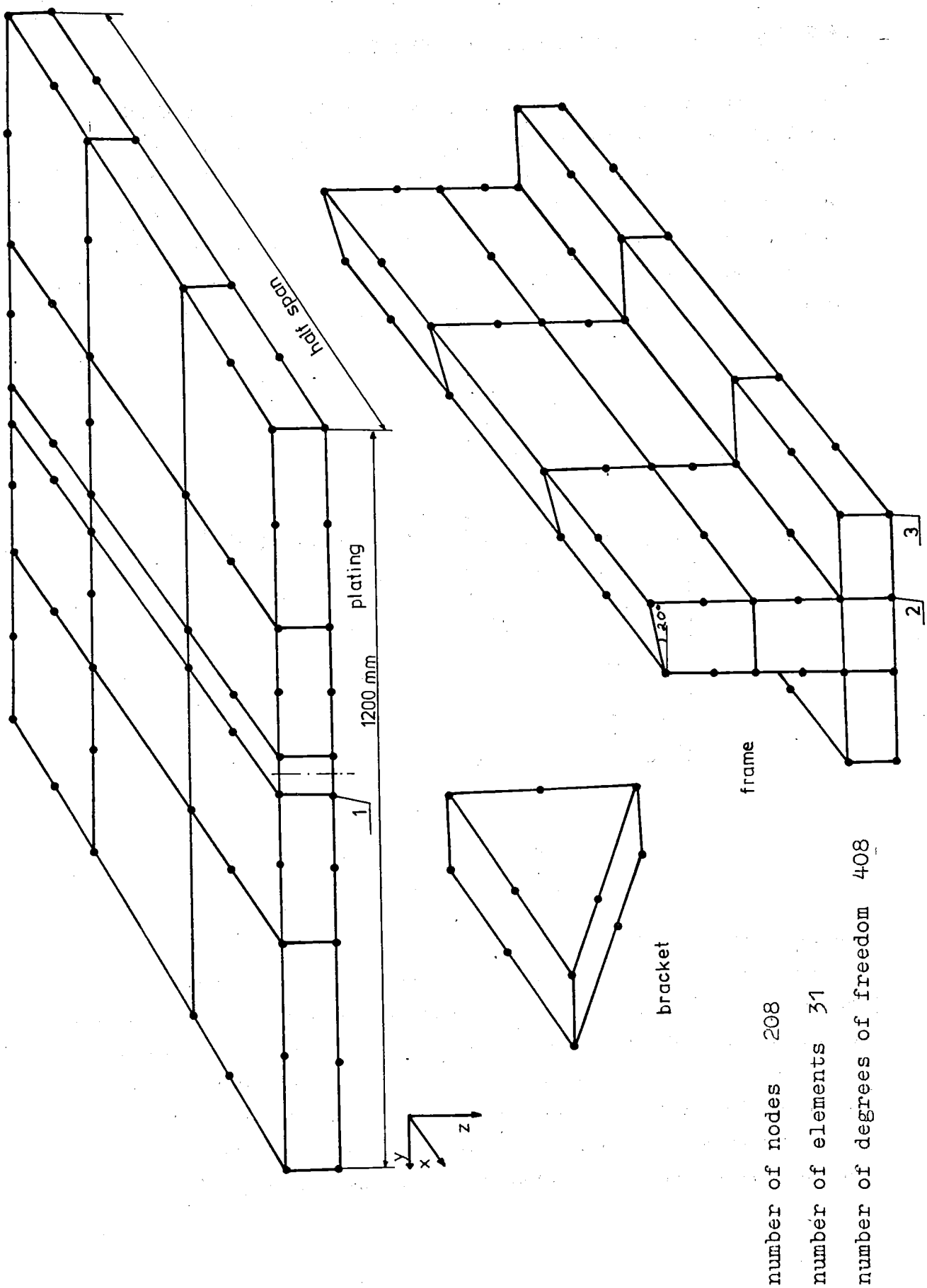

Fig. 18. The finite element model of the ice-strengthened frame structure.

The mesh contains 208 nodes and 31 elements. The number of the degrees of freedom is 408. The load is given as distributed load acting on the elements above the web of the frame. The boundary conditions of the model are such that the structure is clamped at the three edges in all the directions (x,y and z), and in the plane of symmetry the displacements in the direction of the x-axis are restrained.

4.3 Results of the analysis

In the analysis, the load F was gradually increased from 530 kN to 1250 kN as Table 2 shows.

Table 2

Step	1	2	3	4	5	6	7	8	9	10	11
Total load F/kN	530	777	848	900	954	1007	1050	1100	1150	1200	1250

Values of the load F used in the FEM analysis.

The reason for using uneven load steps is to avoid divergence in the iteration procedure of the solution.

The analytic solution showed that the failure of the frame was caused by the shear force at the tip of the bracket. The finite element analysis gives the same result, as can be observed in Fig. 19. It shows the spreading of the plastic areas at each load step. The first plastic zone appears at load F = 848 kN. When the load is increased the plastic area spreads fast through the whole height of the web plate. At load F = 900 kN the web plate is thoroughly plastic. Correspondingly, in the analytic study the plastic limit load was 874 kN. The bracket starts to become plastic at load F = 900 kN.

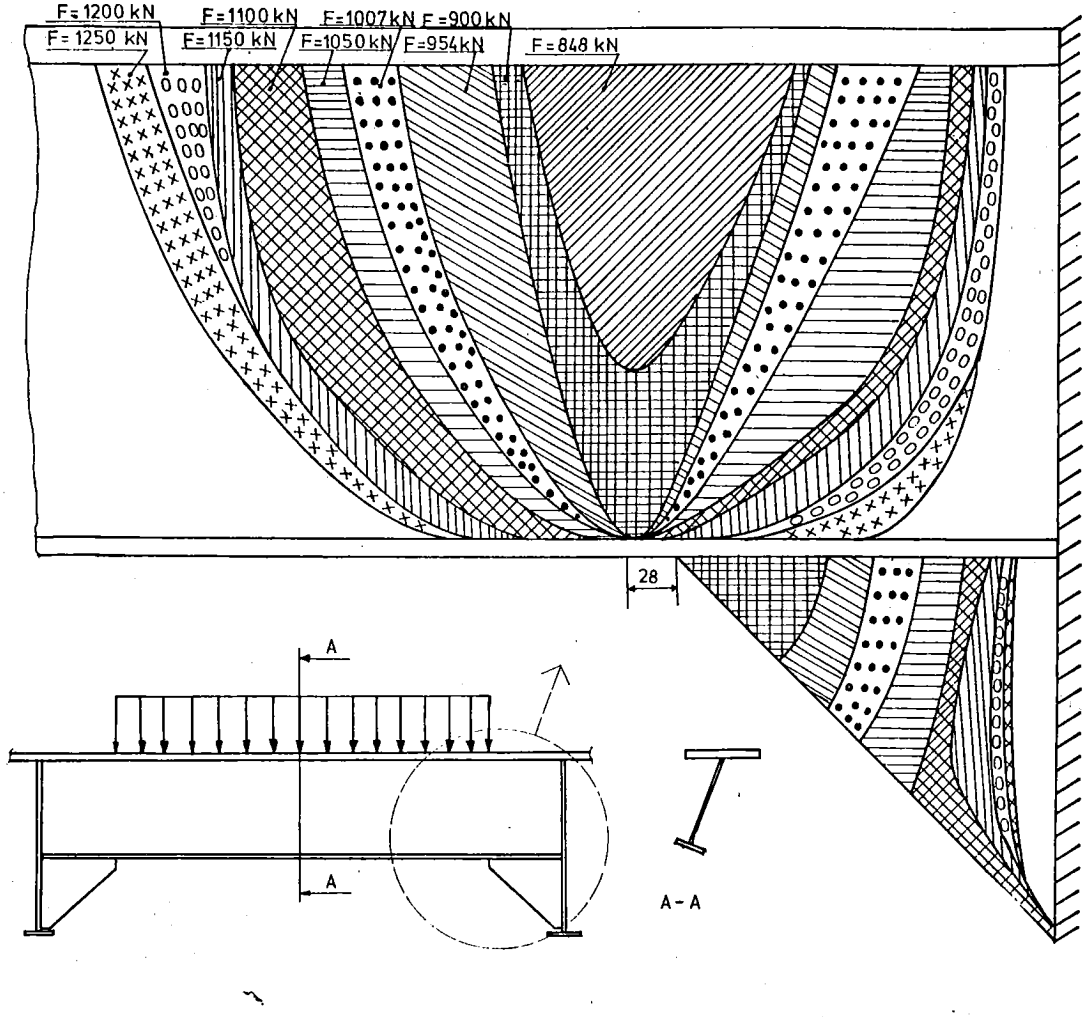

Fig. 19. Plastic zones at different load levels.

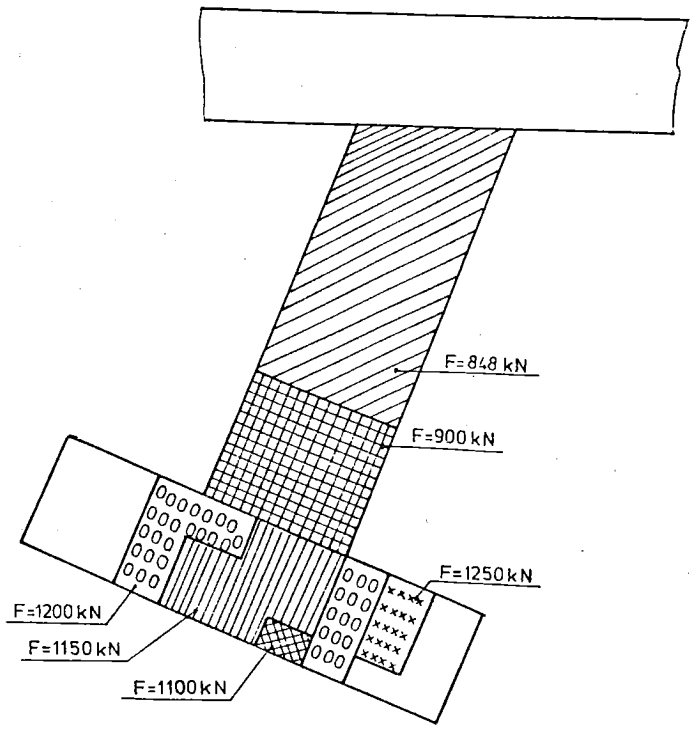

Fig. 20. Plastic zones in the cross section of the frame at a distance of 20 mm from the tip of the bracket towards the centre.

When the load is still increased, the plastic area expands in the longitudinal direction in the web plate. At load F = 1100 kN the flange starts to become plastic as Fig. 20 shows. The formation order of plastic zones in the flange can be explained on the basis of shear lag.

The distribution of shear stress τ_{xz} in the web plate near the tip of the bracket at different load levels is shown in Fig. 21. It can be seen how the shape of the distribution of the shear stress changes when the load is increased. At load F = 900 kN (plastic stage) it is uniformly distributed.

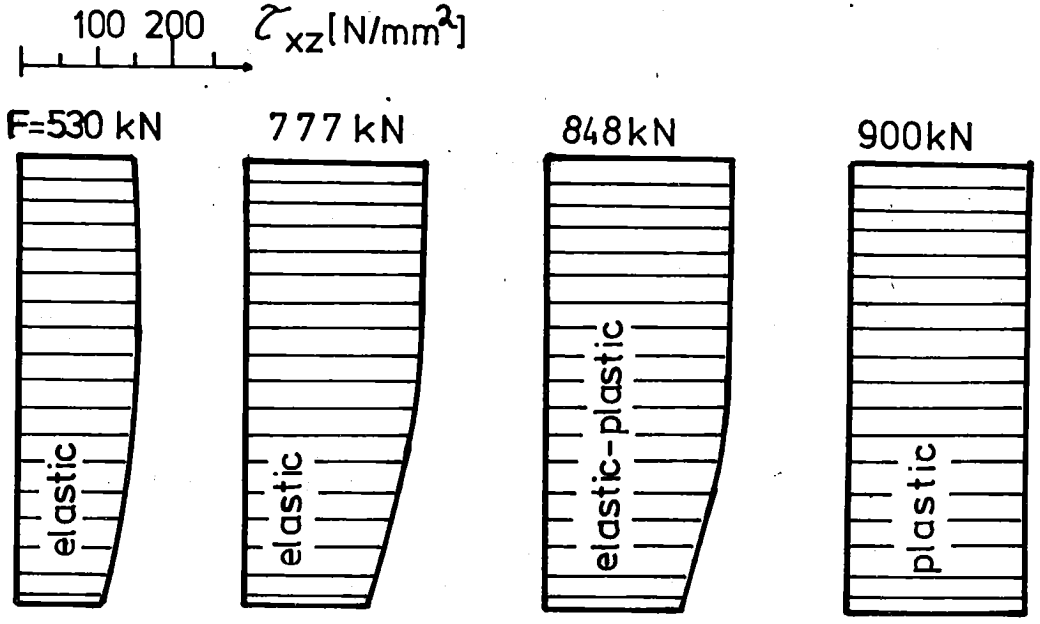

Fig. 21. The distribution of shear stress τ_{xz} at different load levels at the distance of 28 mm from the tip of the bracket towards the centre.

When the cross section of the web plate at the ends is thoroughly plastic, the plating and the flange still have some load carrying capacity, but the displacements both in the vertical and transverse direction will increase rapidly as Fig. 22 shows. The result of the analytic study is also drawn there using the dashed line. It can be seen that the results of these two studies are similar.

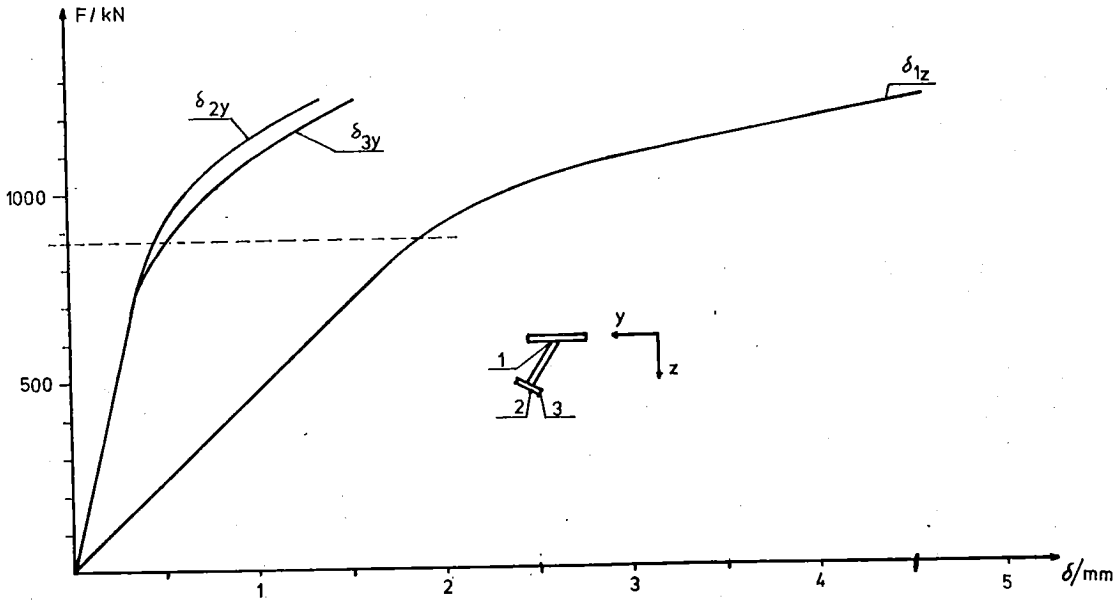

Fig. 22. Load-displacement curves at the midspan of the frame
solid line FEM-analysis
dasked line analytic study

Fig. 22 shows that the distortion of the web plate at the midspan starts at load F = 800 kN when the displacements δ_{2y} and δ_{3y} separate from each other. The deformation pattern of the cross section of the frame at the midspan when load F = 1250 kN is shown in Fig. 23.

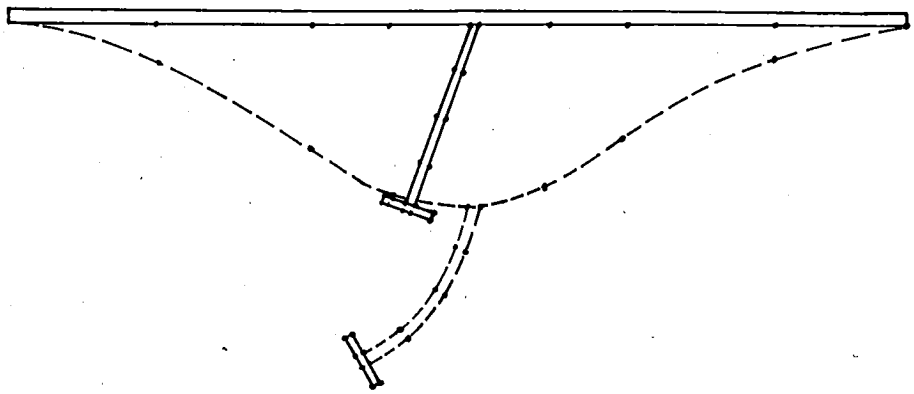

Fig. 23. Deformation pattern of the cross section at load F = 1250 kN.

4.4 Effect of the material properties of the bracket on the load carrying capacity

As the brackets play an important role in the collapse mechanism of the frame, the influence of their material properties on the load carrying capacity of the frame were also studied by changing the yield point from σ_y = 440 N/mm^2 to σ_y = 260 N/mm^2.

Fig. 24 shows the plastic zones at the end of the frame with the weaker bracket at different loads. When making comparisons between this case and that shown earlier in Fig. 19, it is seen that the plastic zones have changed and that the plastic limit load has increased from 900 kN to 945 kN. This increase in the limit load can be explained on the basis that the weaker bracket is capable to take a larger part of the external work than the basic version at the load range where the plasticization of the cross section occurs. As the weaker bracket becomes plastic sooner (at load F = 777 kN) the plastic area in the web plate spreads faster to the end of the frame. The spreading towards the center of the frame is almost equal at both these cases.

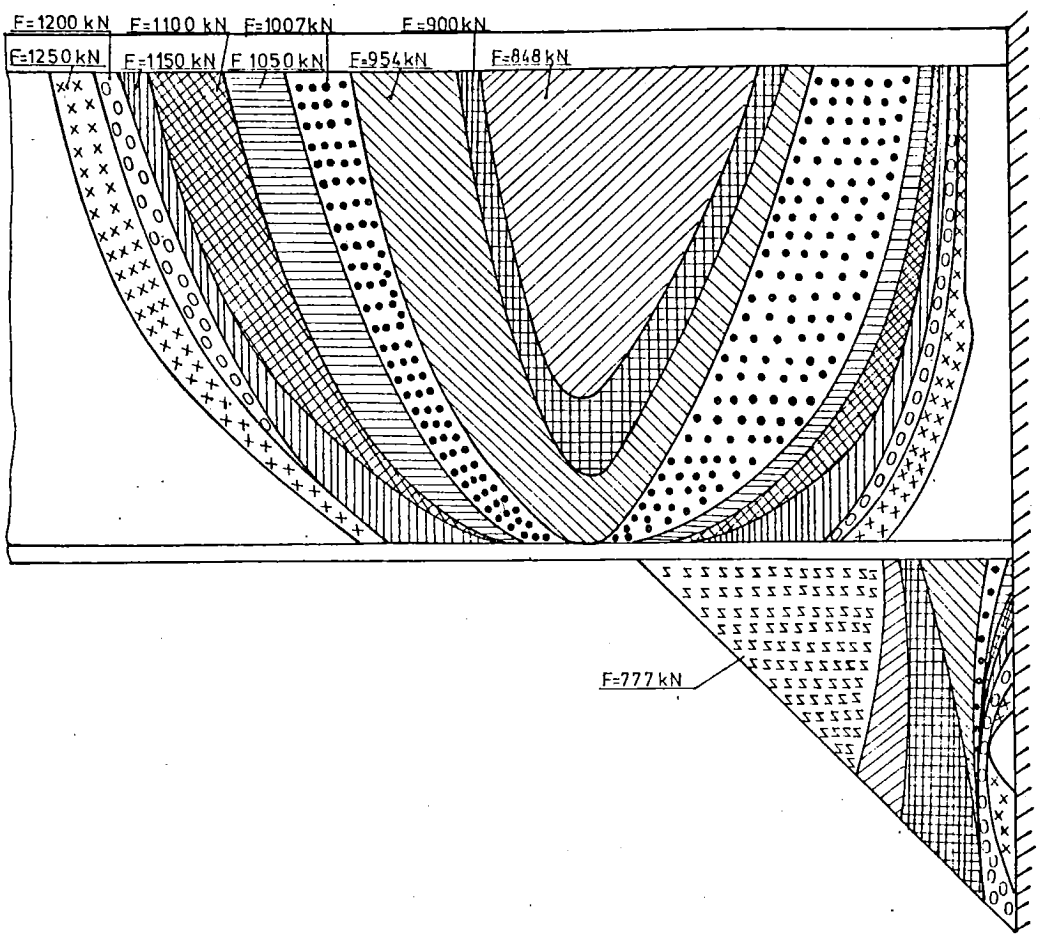

Fig. 24. Plastic zones at different load levels at the end of the frame, when the yield point of the material of the bracket is $\sigma_y = 260\ N/mm^2$.

In Fig. 25 a comparison between the displacements of the frame in these two cases is shown. The reason for that the displacement δ_{2y} is bigger in the basic version is the earlier plasticization of the cross section of the web plate. Thus the behaviour of the web plate has stronger effect on the transverse deflection of the flange than the bracket has. When studying the vertical displacement δ_{1z} the situation is opposite. The weaker bracket causes an increase in the displacement as Fig. 25 shows. In this case the behaviour of the bracket has stronger effect than that of the web plate.

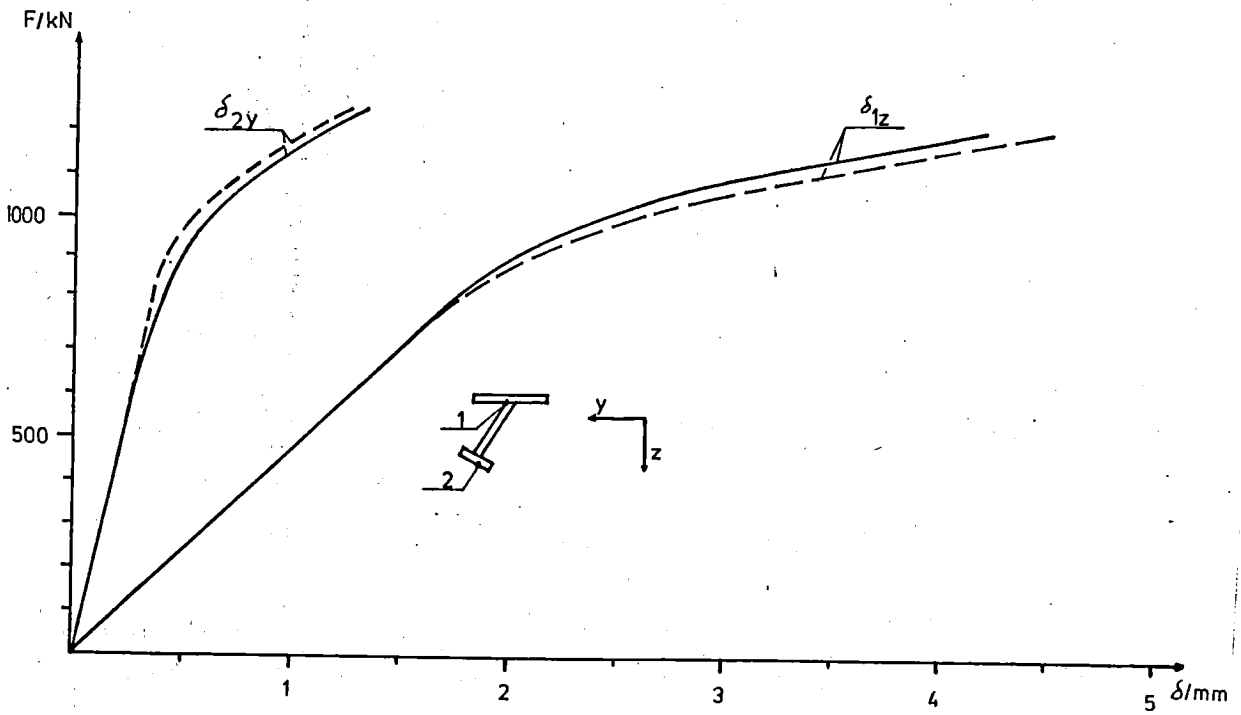

Fig. 25. The effect of yield point of the bracket on the displacements
solid line σ_y = 440 N/mm^2
dashed line σ_y = 260 N/mm^2.

5. MODEL TESTS OF THE STRUCTURE

5.1 Introduction

Two structural tests were performed using the model shown in Fig. 1. A detailed information about the test setup and measuring procedure is given in references /4/ and /11/. Only an overall description about these tests is given in this report. The main aims of these tests from a point of view of this study were to compare the test results with the calculated ones and also to examine the behaviour of the model after the limit load of the frame has been exceeded.

The reason why two tests were made is that at the first one the maximum load was too small to cause the failure of the loaded frame. This arose from the higher yield-stress levels of the material used in the model than was supposed and from inaccuracies in calculations made beforehand. The arrangement of the test system was principally equal in both cases.

5.2 Measuring system

In the first test the model was loaded by two 50 tons cylinders and in the second one by a 1000 ton press machine. Fig. 26 shows overall views of the first and second test. The force from the piston was acting at two points and it was divided into four points by beams and steel pieces as Fig. 27 shows. In this way the load distribution was more uniform. The longer sides of the model were fastened to the foundation with bolts.

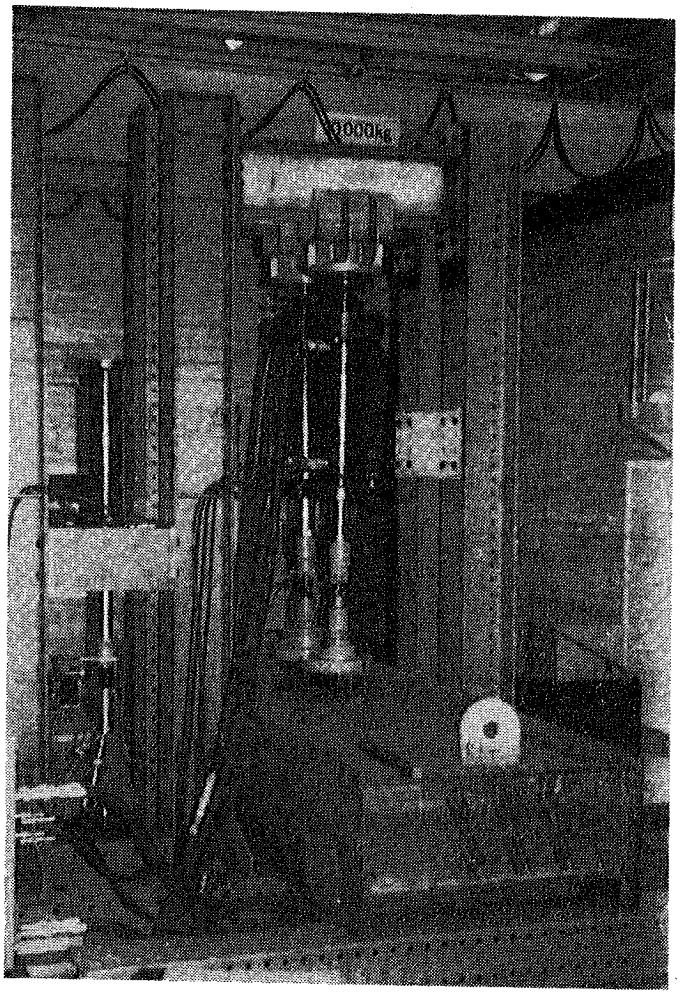

First test

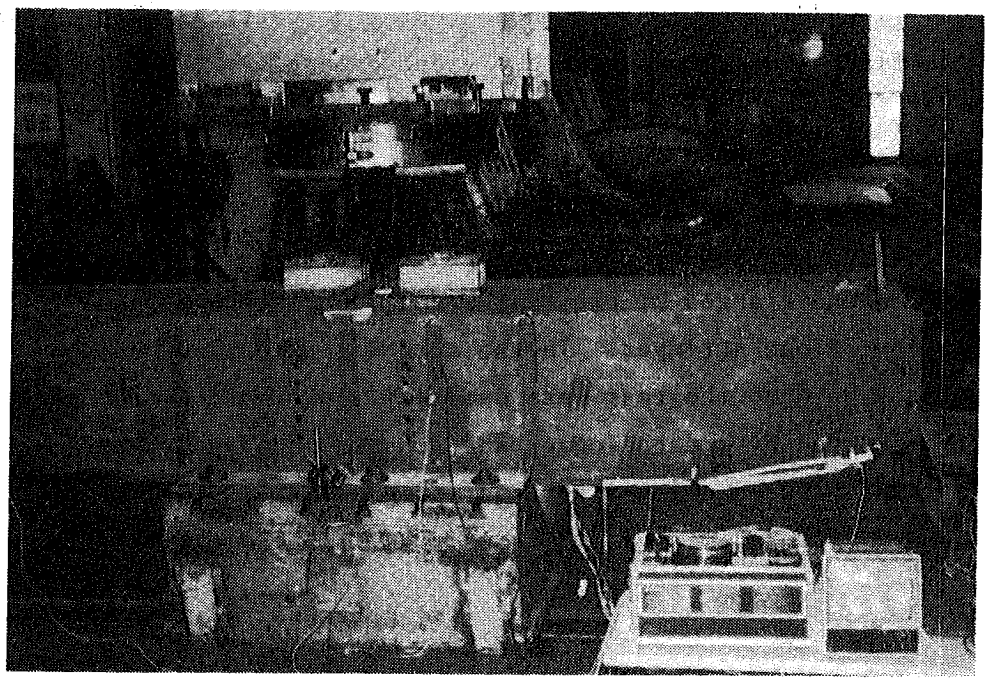

Second test

Fig. 26. An overview of the tests.

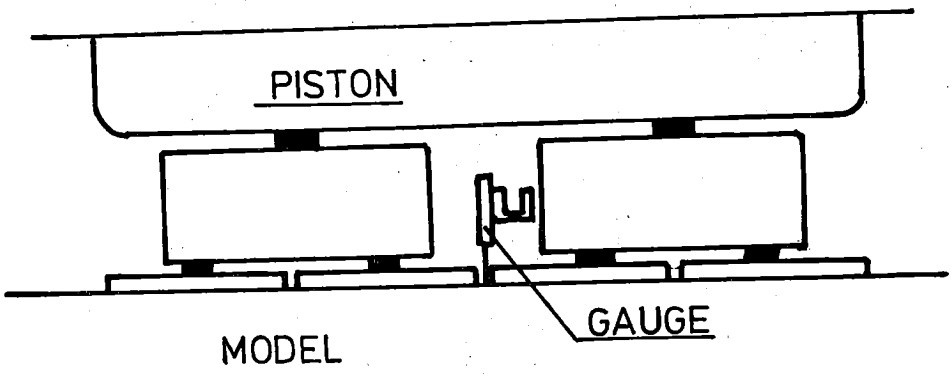

Fig. 27. The loading arrangement of the model.

The following quantities were measured during the tests:

- total load, in the first test with force pick-ups and in the second one with an electric pressure gauge. In the first test the load range was from 0 to 100 kN and in the second from 120 kN to 300 kN.

- vertical displacement of the plating at the midspan of the loaded frame and transverse displacement of the flange of the frame were measured with displacement gauges as Fig. 28 schematically shows. In addition, in the second test, the vertical displacement of the flange was recorded with a video camera.

- stresses using strain gauges, the places of which are shown in Fig. 29 /4/. The total number of these was 42, consisting at nine rosette gauges on the web plate of the middle frame, nine gauges on the flanges of the frames and two rosette gauges at the web plate of one stringer. In the second test only 38 of them were used because the rest were damaged. Information from gauges was registered by a data logger and punched on paper tapes and afterwards handled using a computer program.

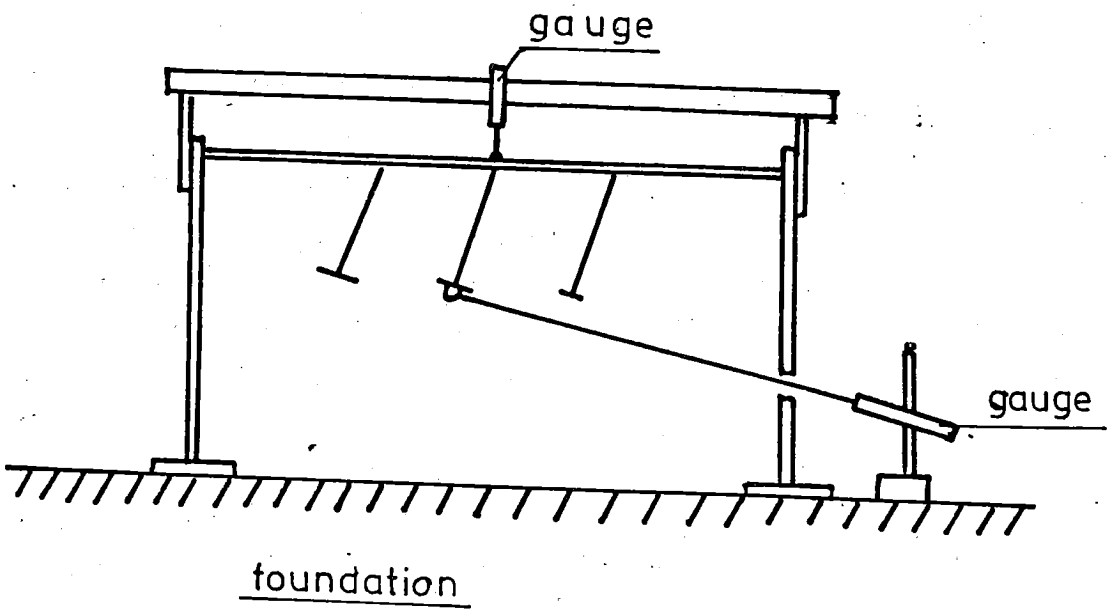

Fig. 28. The deflection measuring system of the frame with ~~displacement~~ gauges.

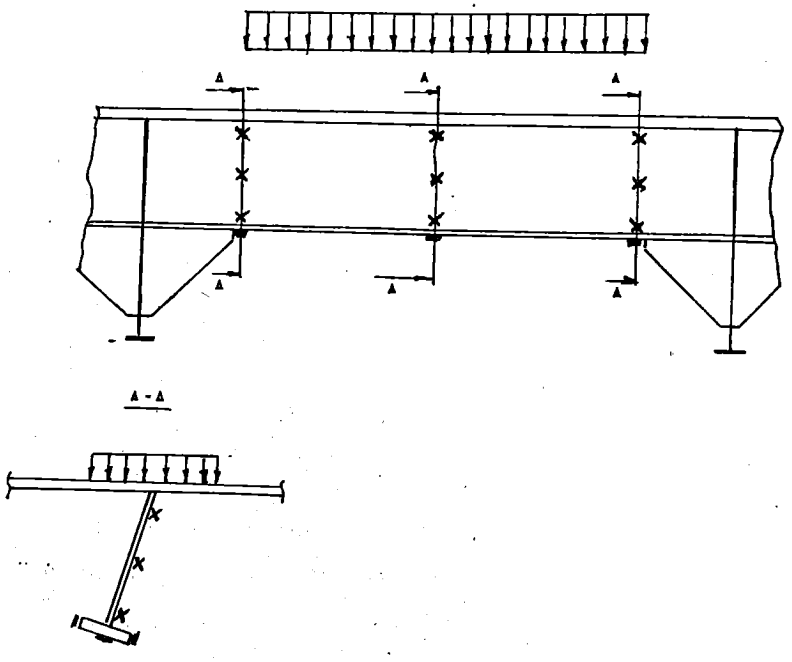

Fig. 29. The stress measuring points /4/.

5.3 Comparison between measured and calculated results

This chapter deals with those test results which have interest from a point of view of comparing them with the calculated ones. In this sense the deflections of the middle frame and shear stresses at the web plate of the middle frame are the most interesting variables.

Fig. 30 shows the measured and calculated force-displacement curves. As the test model differs in some points from the one used in the calculations the index 1 is added into the symbol of the load to avoid confusion. The solid curves represent the measured ones. The ends of these curves are drawn with dashed lines because these are obtained from the second test.

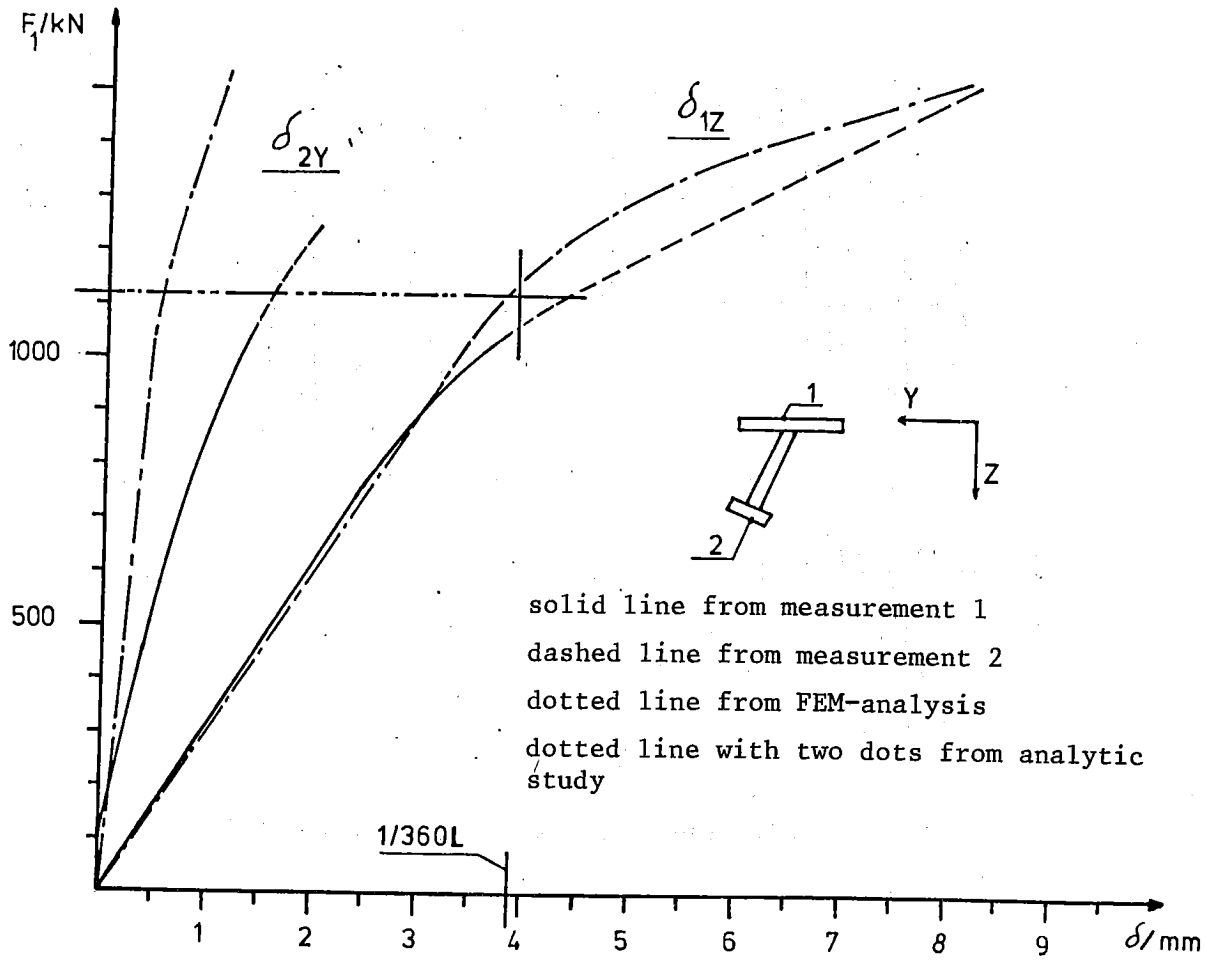

Fig. 30. Comparison between measured and calculated load-displace curves.

The dotted curves in Fig. 30 are derived from the results of the FEM-analysis by making some corrections which arise from the differences between the test and calculation model. These differences are shown in Table 3. The correction factors by which the calculated results are multiplied have been obtained from the calculations performed with linear FEM-models.

Table 3.

Item	Calculation model	Test model	Correction factor
End connection of the frame	Clamped	Frame continues one stringer spacing in both directions	Displacement 2.03
Number of frames	One	Three	Load · 1.25
Load distribution	Line load	Load width 100 mm	Load · 1.03

The differences between the test and calculation model.

The corrected result from the analytic study is drawn in Fig. 30, two. Then comparing the measured and calculated curves the following viewpoints can be stated:

- the calculated curve of the vertical displacement δ_{1z} reaches on about 15 % higher load level before becoming non-linear than the measured one

- discrepancy in the transverse displacement δ_{2y} is due to the fact that the deformed shape of the cross section of the loaded frame is different in the test and in the FEM-analysis as Fig. 23 and 34 show. This may arise from the different end supports of the flange. In the calculation it was clamped while in the test it was free as Fig. 1 shows. So in the first case the rigidity of the flange against transverse bending was bigger.

The curves of Fig. 30 clearly show that the structure is not in a state of real collapse, when the plastic limit load of the frame is reached. As the material of the structure behaves as a ductile one the deflections will also play an important role in this problem. The deflection which is 1/360 of the span of the frame /8/ is also drawn in Fig. 30.

Fig. 31 shows the measured and calculated distributions of shear stress τ_x near the tip of the bracket at load F_1 = 940 kN. The reason for some differences between these distributions may be due to local disturbancies at the measured ones as the strain gauges were glued only on one side of the web plate.

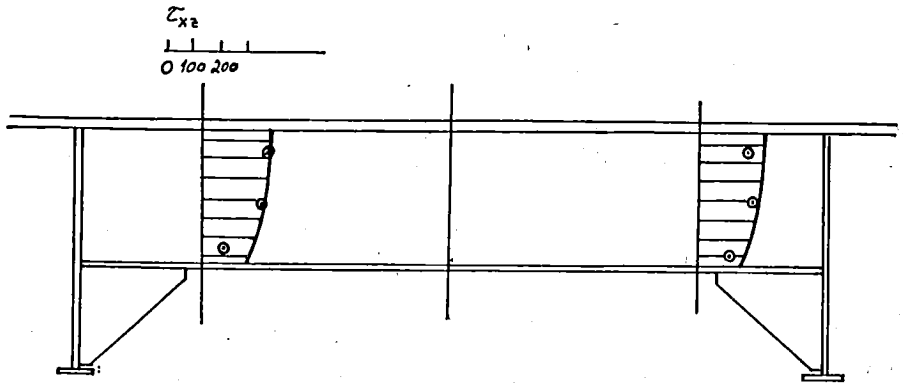

Fig. 31. Comparison between measured and calculated shear stress distributions load F_1 = 940 kN.

5.4 Behaviour of the frame beyond the plastic limit load

In the previous chapters it was observed that the plastic limit load of the frame was reached when the web plate had become thoroughly plastic. It can be intuitively detected that in spite of this the frame still carries the load with its flanges and that the plating effectively distributes the load to the other strength elements. This behaviour of the structure can be studied

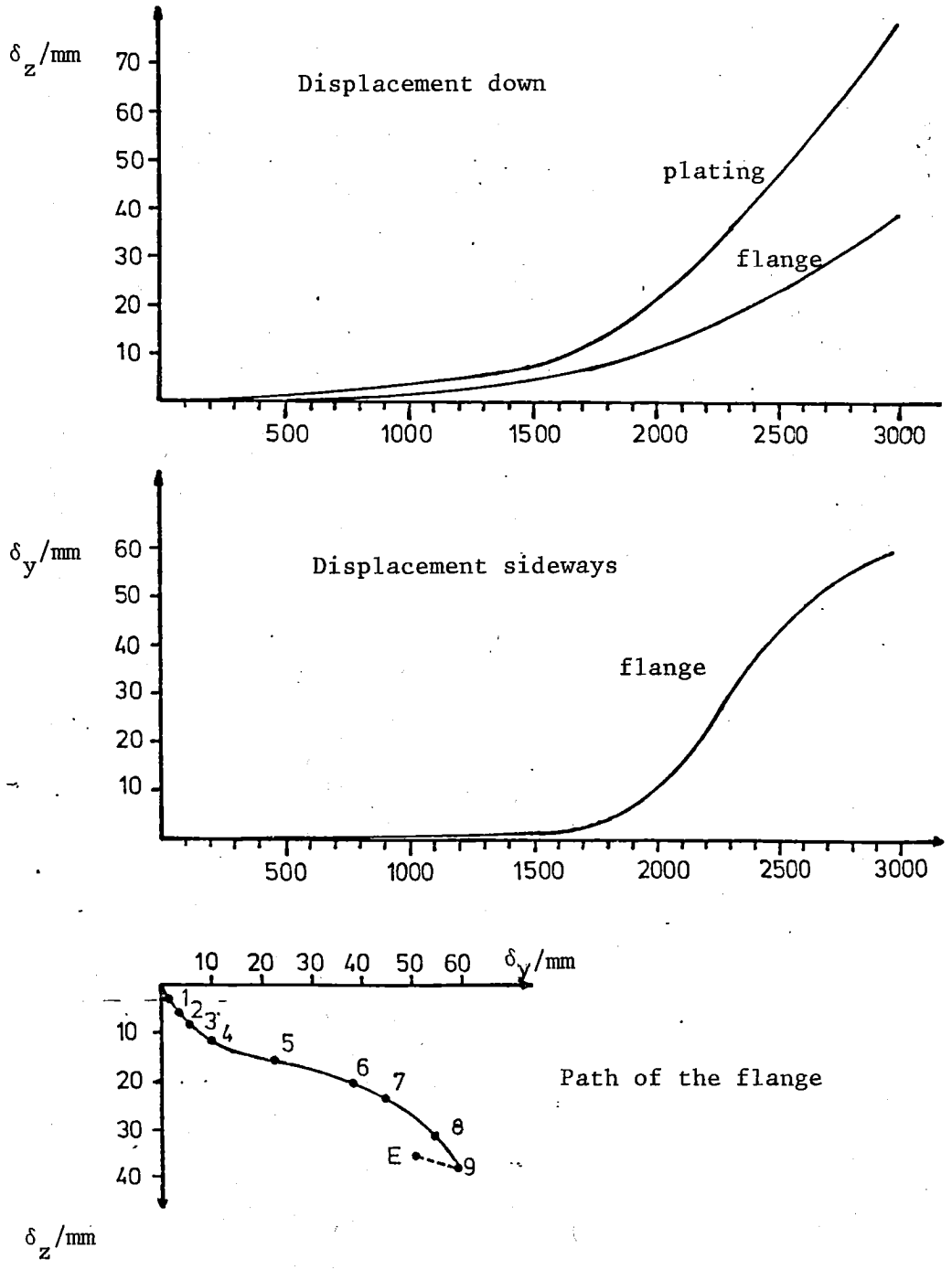

Fig. 32. Measured load-deflection curves.

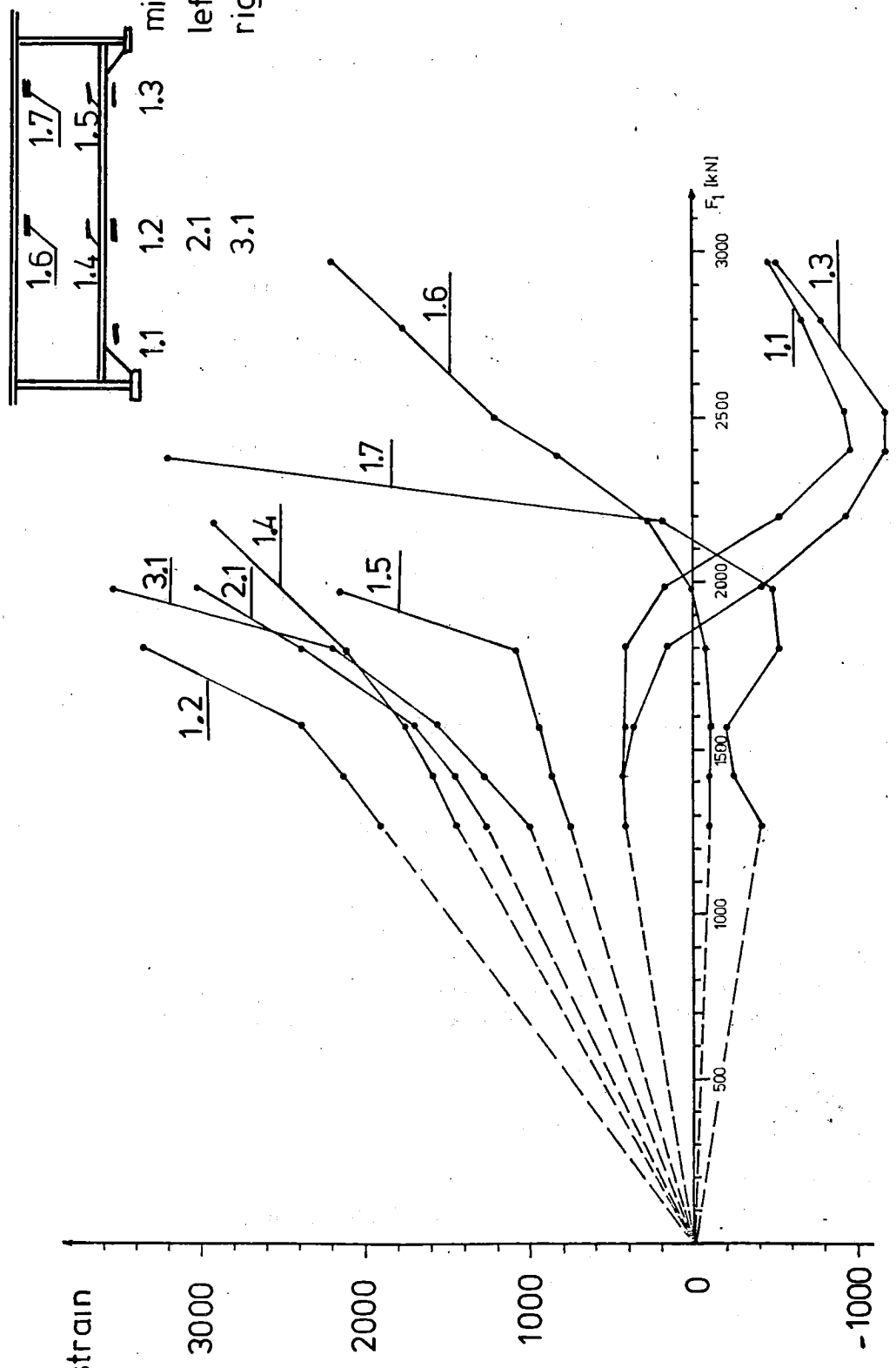

Fig. 33. Strain in the frames as a function of the load.

most easily using a structural model test as, for instance, by means of a FEM-analysis if might be too laborius and expensive to investigate.

In the following some results from the second test /11/ are represented. Fig. 32 shows the deflections of the loaded frame in the vertical and transverse directions. It shows also the track of the flange. When the load reaches about 1800 kN, the deflections in both directions start to increase more rapidly, and the vertical displacements of the plating and flange differ more from each other, which means that the web plate deforms heavily. At the same time the strain in the flange near the tip of the bracket changes its sign from tension to compression as Fig. 33 shows. So the two unloaded spans of the frame start to counteract, which leads after some time, when the load is still increased, to clamping of some degree, and the increase of the vertical deflections is stabilized. Fig. 33 also shows how the normal stresses at the cross section of the midspan behave. A plastic hinge develops there and it is fully developed at a load of about 300 kN.

Fig. 34 shows the deformation pattern of the cross section of the frames after the experiment. When comparing it to ice-induced casualties in a real shell structure the patterns are quite similar. In fig. 35 are photographs taken from the model after the experiment. The first one shows how the frames have bent in the lateral direction, and the second one shows the deformation pattern of the brackets.

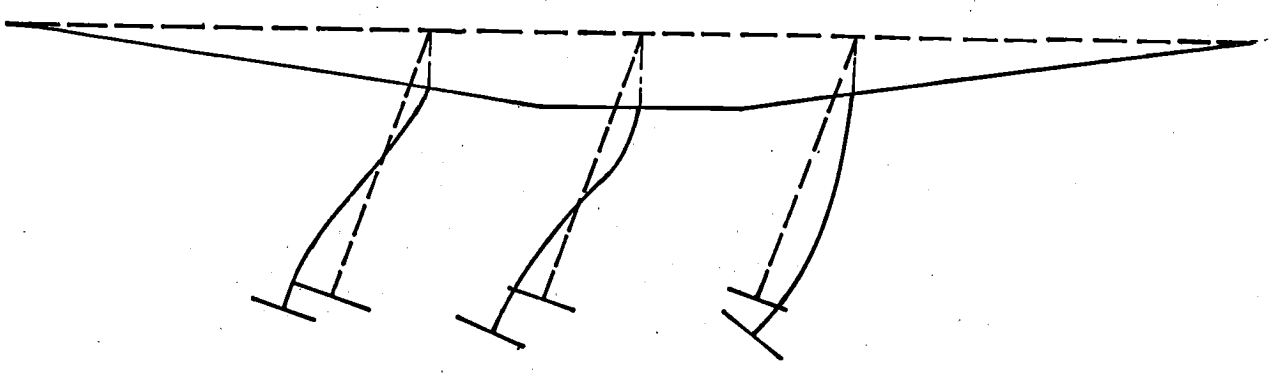

Fig. 34. The deformation pattern of the cross section after the experiment.

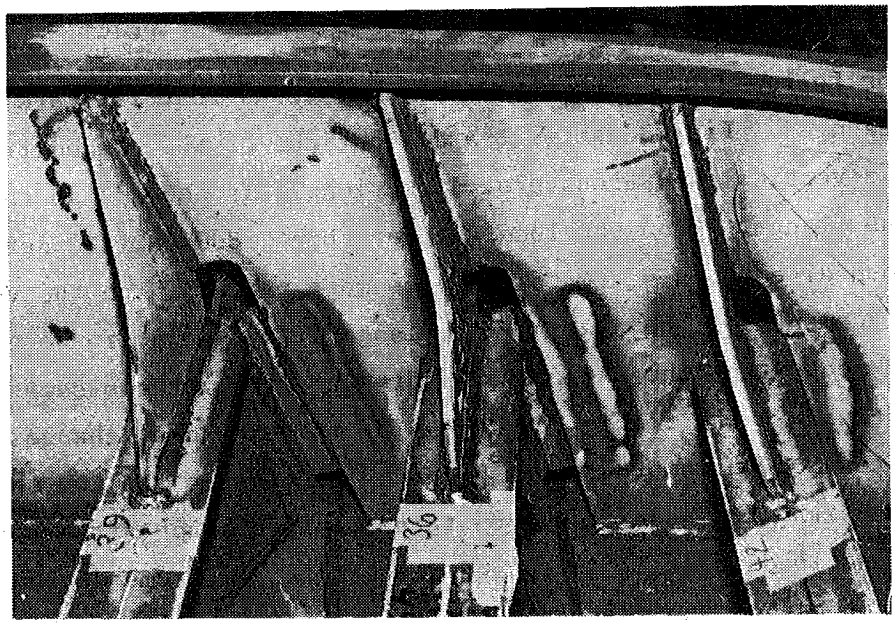

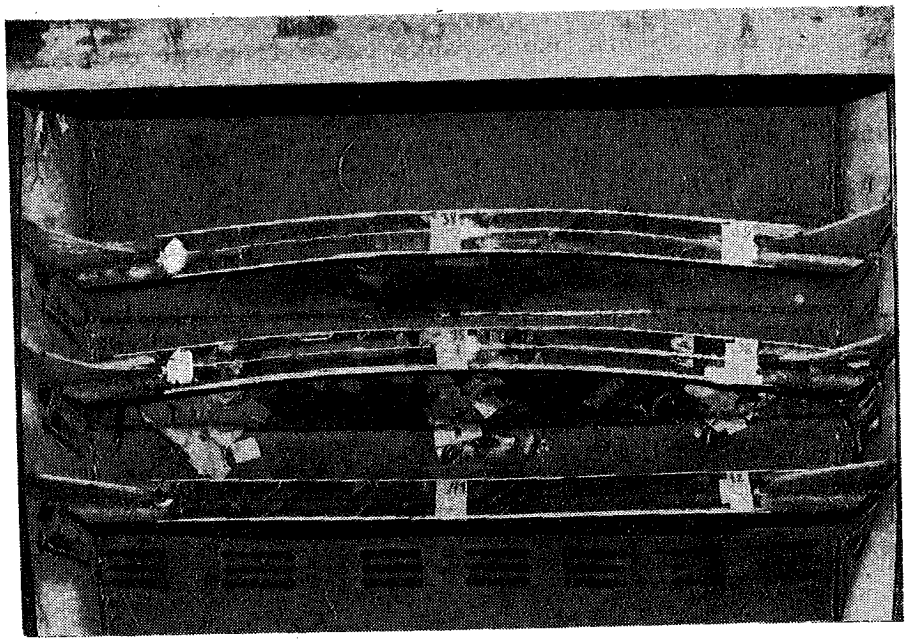

Fig. 35. The model after the experiment.

6. CONCLUSIONS

This work includes both theoretical calculations using plastic design theorems, the finite element method, and an experimental study with a model test. The analytic treatment showed its advantages: with a small amount of computation it is possible to obtain results which are for practical use reliable enough. In spite of the fact, that with the finite element method using a thick shell element it is possible quite accurately to study both stresses and deflections, its disadvantage is clearly that a nonlinear analysis needs a lot of computer time and a large central memory. Therefore the problem in question must be simplified. A model test, of course, gives as such the most reliable results but the difficulty lies often at the modelling technique of a non-linear phenomenon.

Both the calculations and experiments showed that the collapse process of the frame occurs in many phases due to the ductilty of the material and not at once after reaching the plastic limit load. The study demonstrates that the frame structure has a quite big plastic reserve after the limit load. Of course the question of permanent deflections is then brought into discussion.

The replacement of the complicated load pattern with such a simple one is an obvious drawback but today the lack of data from full-scale measurements does not give any other choice. It is hoped that the long-term ice pressure measurements which are going on in the Baltic Sea will give more data for a more representative load pattern.

7. ACKNOWLEDGEMENT

The authors wish to express their warm gratitude to Professor J-E. Jansson, at present the director general of The Finnish Board of Navigation, for his encouraging support and valuable advices during the work.

The authors also tank Oy Wärtsilä Ab Helsinki Shipyard for their co-operation in conduction the experimental phase of this work. Especially the assistance of Mr. S. Korppoo and Mr. P. Tuovinen is warmly appreciated.

The authors want to express their appreciation for the valuable help of the staff of the Laboratory of the Strength of Materials at the Helsinki University of Technology.

Our thanks are also due to the staff of the Ship Laboratory at the Technical Research Centre of Finland. Especially the assistance of Mr. P. Kujala and Mr. J. Vuorio is warmly appreciated.

Financially this work has been supported by the Winter Navigation Research Board.

8. REFERENCES

/1/ Varsta P., Measurement and analysis of ice-induced stresses in the shell of an icebreaker. The Winter Navigation Research Board. Research report 21. Helsinki 1977.

/2/ Hakala M., Riska K., Varsta P. & Vuorio J., On ice-induced stresses in the shell of the icebreaker Teuvo. VTT Ship Laboratory. Research report (unpublished). Helsinki 1978.

/3/ Johansson B.M., On the ice-strengthening of ship hulls. ISP 14(1967). 154 s. 321...245.

/4/ Ranki E., Study on stability of frame of an icebreaker (in Finnish). The Helsinki University of Technology. MSc. (Tech.) thesis. Helsinki 1976.

/5/ Tension tests according to SFS 3173. VTT Metals Laboratory. Otaniemi 1977. (Unpublished.)

/6/ Droumev I.V., Application of ultimate load method in ship structures. Lectures given at The Helsinki University of Technology. Helsinki 1976.

/7/ Bathe K-J., ADINA-finite element program for automatic dynamic incremental nonlinear analysis. Massachusetts Instutute of Technology. Cambridge, Massachusetts 1976.

/8/ Plastic design in steel, a guide and commentary. ASCE-manuals and reports on engineering practice- no. 41. Second edition. New York 1971.

/9/ Faulkner D., A review of effective plating for use in the analysis of stiffened plating in bending and compression. JSR 19 (1975) 1, s. 1...17.

/10/ Neal B.G., Plastic Method of structural analysis. Great Britain, Chapman & Hall Ltd, 1970.

/11/ Vuorio J., A model test of an icebreaker shell at Wärtsilä Helsinki Shipyard. VTT Ship Laboratory. Research report. Espoo 1978. (Unpublished.)

ISBN 951-46-3756-9